Original Research

Characterization of porcine pregnane X receptor, farnesoid X receptor and their splice variants

Matthew A Gray[1], Callie B Pollock[2], Lawrence B Schook[2] and E James Squires[1]

[1]Department of Animal and Poultry Science, University of Guelph, Guelph, Ontario, Canada N1G2W1; [2]Department of Animal Sciences, University of Illinois at Urbana-Champaign, Urbana, IL 61801, USA
Corresponding author: Dr E James Squires. Email: jsquires@uoguelph.ca

Abstract

The pregnane X receptor (PXR; NR1I2) and the farnesoid X receptor (FXR; NR1H4) regulate the expression of many major metabolic enzymes. With the pig being used as a model for humans in metabolic and toxicological studies and also an important food animal, we characterized the transactivation profile of the porcine orthologs of these receptors, pgPXR and pgFXR. We compared the transactivation profiles of these receptors and their splice variants to their human orthologs using mostly endogenous ligands. Five alternatively spliced variants were identified for pgFXR as part of this study, while five alternatively spliced variants of pgPXR had been previously described. Insertions and deletions within these splice variants generated truncated proteins or proteins with altered tertiary structures, resulting in altered transactivation. Realtime polymerase chain reaction analyses showed that the pgPXR variants were present in liver cDNA samples from 3.33% to 7.92% of the total pgPXR, while the pgFXR variants were present from 1.92% to 9.26% of the total pgFXR. pgFXR was fairly evenly expressed in seven different tissues. In a luciferase reporter assay, wild-type pgPXR (pgPXR-WT) and human PXR (hPXR) responded to 12 common ligands, with similar levels of activation occurring for six of these. Wild-type pgFXR (pgFXR-WT) significantly responded to three ligands, two of which also activated hFXR. 3-Methylindole (skatole) was identified as a novel inverse agonist for pgPXR-WT and pgFXR-WT as well as porcine constitutive androstane receptor. None of the pgPXR splice variants (SVs) were active in the luciferase reporter assay on their own; pgFXR-SV1 was activated by chenodeoxycholic acid to a similar degree as pgFXR-WT. When co-transfected with their corresponding wild-type proteins, pgPXR-SV1 and pgFXR-SV1 significantly increased receptor transactivation. In conclusion, pgPXR-WT and pgFXR-WT both responded to ligands that activated their human orthologs, and some of the alternatively spliced variants significantly altered pgPXR and pgFXR transactivation at *in vivo* expression levels.

Keywords: nuclear receptor, PXR, FXR, splice variants, gene expression

Introduction

Nuclear receptors are a class of transcription factors that are intimately involved in the regulation of a wide variety of metabolic processes, including synthesis of endogenous compounds and metabolism of both endogenous and exogenous substances. In total, 49 members of this family of transcription factors have been identified in humans.[1] Nuclear receptors are modular proteins, containing a number of domains that are conserved with variable consistency throughout the family. At the N-terminus there is a highly variable domain that contains the conserved AF-1 motif, which is implicated in ligand-independent transactivation. Next is the DNA binding domain (DBD), which consists of two zinc fingers; this is followed by another highly variable hinge region. C-terminal to the hinge region is the ligand binding domain (LBD), which contains within its C-terminal end the AF-2 domain involved in ligand-dependent transactivation.[1] The C-terminal end of the protein is also involved in protein–protein binding, for a number of nuclear receptors form homo- or heterodimers upon activation by ligands.[2]

A subset of the nuclear receptor family, the Class II nuclear receptors, forms heterodimers with the retinoid X receptor (RXR) upon ligand activation.[3] In this class of receptors are the farnesoid X receptor (FXR) and pregnane X receptor (PXR). FXR has been identified as the hepatic bile acid receptor that regulates the expression of genes involved in bile acid transport and synthesis.[4] There is some evidence that FXR is not restricted to its role as a bile acid receptor, since 5α-androstan-3α-ol-17-one

(androsterone), a weak androgen, is capable of activating FXR.[5] FXR may also be linked to general hepatic metabolic processes, for it has been shown to cause up-regulation of hydroxysteroid sulfotransferase (SULT2A1)[6,7] and PXR,[8] both of which are involved in metabolism of a wide variety of endogenous and exogenous compounds. FXR has been cloned and characterized in a number of species including human, rat[4] and mouse,[9] although it has yet to be cloned and characterized in the pig.

The PXR is one of the major xenobiotic sensing nuclear receptors expressed in the liver, along with the constitutive androstane receptor (CAR), to which it is closely related.[10] The LBD of PXR is extremely large, allowing for a wide array of exogenous and endogenous compounds to act as activating ligands.[11] Evolutionary changes in the LBD have resulted in differential responses to common ligands and altered ligand specificity among different species.[12,13] Upon activation, PXR regulates the expression levels of many major metabolic enzymes, including the cytochrome P450 family of phase I enzymes and various families of phase II enzymes.[14–16] PXR has been extensively studied in many species, including human and mouse. The coding sequence for pig PXR (pgPXR) has been determined,[17] although characterization of activating ligands has yet to be carried out.

Alternatively spliced variants of nuclear receptors have been shown to have various effects on the transactivation of the wild-type receptor. Splice variants identified for mouse CAR have lost their transactivation ability due to the loss of the C-terminal end of the LBD and the transactivation (AF-2) domain.[18] Human CAR variants have been identified in which amino acid insertions occurred; these retained transactivation abilities, but with a decreased efficiency compared with the wild-type protein.[19–22] Alternatively spliced nuclear receptor variants can sometimes attenuate the transactivation of the wild-type protein, which is termed a dominant-negative effect.[23] This effect has been exhibited by rat CAR, mouse PXR and rat FXR that had their AF-2 domains artificially deleted.[24] Naturally occurring dominant-negative splice variants have also been found; variants of peroxisome proliferator-activated receptor γ inhibit the transactivation of the wild-type protein by preferentially binding nuclear co-factors.[25] A dominant-negative effect has also been shown in pigs, with a pig CAR variant being found to significantly decrease the transactivation of the wild-type receptor *in vitro*.[26] The opposite effect, a dominant-positive effect, has also been shown, with an alternatively spliced variant of the estrogen receptor causing a significant increase in wild-type receptor transactivation.[27]

The use of pigs as a biomedical research model has been gaining increased interest in recent years.[28] The basis of this interest is pharmacological and toxicological studies comparing pigs to humans, and as such an understanding of how specific liver nuclear receptors differ between the two species is required. Our objective was to determine the transactivation profile of pgPXR and pgFXR, particularly with endogenous ligands that are present in the pig. The expression levels of pgFXR in seven tissues were determined, for this is the first report of pgFXR being cloned, and

tissue distribution of this receptor was previously unknown. We also compared the transactivation profiles of pgPXR and hPXR as well as pgFXR and hFXR, using dual-luciferase assays. We hypothesize that due to sequence similarities at both the gene and protein levels, the human and pig orthologs of each receptor are likely to respond to similar ligands. Alternatively spliced variants found through the course of cloning pgFXR and pgPXR[17] were also tested for individual transactivation, as well as for potential effects on the activities of the wild-type proteins. The expression levels of each of these variants, as a percentage of total pgFXR or pgPXR, were also determined in liver tissue of domestic pigs.

Methods and materials

Research animals

Animals used for the cloning and characterization of pgPXR and pgFXR were obtained from the Arkell Swine Research facility of the University of Guelph. Procedures were approved by the Animal Care Committee at the University of Guelph and used in accordance with the guidelines of the Canadian Council on Animal Care. Pigs were uncastrated Yorkshire males weighing approximately 100 kg and were slaughtered in the abattoir, University of Guelph. Livers, small intestines, lungs, hearts, kidneys, adrenal glands and testes were removed immediately following the slaughter and used for extraction of RNA. Total RNA was isolated from the tissue using Tri-Reagent (Sigma Chemical Co, St Louis, MO, USA) and reverse transcribed using SuperScript II with oligo dT primers (Invitrogen Corp., Burlington, ON, Canada) to produce cDNA.

Cloning of Pig PXR and its splice variants

pgPXR was amplified from porcine liver cDNA using the forward and reverse primers 5′ GCC<u>ATG</u>CAATGCAATG AAACAGA 3′ and 5′ TCAGCTTTCTGTGATGC 3′, respectively. These primers were designed to amplify the pgPXR coding sequence from the reference sequence (Genebank accession no. NM_001038005). pgPXR was amplified using Platinum *Taq* DNA Polymerase High Fidelity (Invitrogen Corp.) with the following program: (94°C, 2 min (94°C, 30 s; 63°C, 30 s; 68°C, 1.5 min) × 35 cycles; 68°C, 10 min). The resulting polymerase chain reaction (PCR) product was gel purified and ligated into the pcDNA3.1/V5-His TOPO vector (Invitrogen Corp.) following the manufacturer's instructions. The isolated plasmids were sequenced to identify an expression plasmid containing the complete pgPXR expression sequence, termed pgPXR-WT.

Splice variants of pgPXR were cloned as previously described.[17] Each splice variant (pgPXR-SV1 through pgPXR-SV5) was subcloned into the pcDNA3.1/V5-His TOPO vector. The expression plasmids were sequenced to confirm they contained the proper coding sequences for each of the alternative splice variants.

Cloning of porcine FXR and its splice variants

A putative pgFXR sequence was assembled from porcine expressed sequence tags (ESTs) using the human FXR reference sequence (Genebank accession no. NM_005123) as a template. From this sequence, the forward and reverse primers 5′ GCCATGGTAATGCAGTTTCAGG 3′ and 5′ GGAGGAAAATGAAGAGCTAGA 3′ were designed to PCR amplify the pgFXR coding sequence using Platinum *Taq* DNA Polymerase High Fidelity (Invitrogen Corp.) with the program (94°C, 2 min (94°C, 30 s; 64°C, 30 s; 68°C, 1.5 min) × 35 cycles; 68°C, 10 min). The resulting PCR product was purified on a 1% agarose gel and TA cloned into the pcDNA3.1/V5-His TOPO vector (Invitrogen Corp.) following the manufacturer's instructions. All plasmids were sequenced to ensure that the correct coding sequence for pgFXR had been isolated, termed pgFXR-WT. During the plasmid sequencing, five alternatively splice variants of pgFXR-WT were also isolated and these were named pgFXR-SV1 through pgFXR-SV5.

Realtime PCR

The relative amounts of mRNA for each of the pgPXR and pgFXR splice variants, as well as the total amounts of pgPXR and pgFXR, were determined in RNA isolated from the livers of 10 individual Yorkshire pigs and converted to cDNA as described previously. Realtime PCR primers were designed using PrimerQuest (Integrated DNA Technologies, http://www.idtdna.com/Scitools/Applications/Primerquest/) for each of the pgPXR and pgFXR variants, as well as for total pgPXR and total pgFXR (Table 1). Primer design, specificity testing and determination of amplification efficiencies were carried out as described by Gray *et al.*[26] Tissue distribution for pgFXR was also determined in seven tissues (liver, small intestine, lung, heart, adrenal gland, kidney and testes) using the Total pgFXR primers from Table 1.

Realtime PCR was carried out as described previously[26] using the qPCR program as follows: (94°C, 10 min (94°C, 15 s; 64°C, 30 s; 72°C, 30 s; 75°C, 15 s) × 40), with fluorescence being recorded during the 75°C step. Melt curves from 72 to 94°C were produced during each experiment to confirm the presence of a single product. Relative fold expression of each gene was calculated using the $2^{-\Delta\Delta CT}$ method[29] using a positive control sample containing 0.01 ng of the corresponding plasmid for the splice variant primer set being used.

Activities of pgPXR-WT, hPXR, pgFXR-WT and hFXR using the luciferase reporter assay

For transactivation assays for each of the four wild-type nuclear receptors to be tested (pgPXR-WT, hPXR, pgFXR-WT and hFXR), HepG2 cells were cultured in Eagle MEM (Earle's balanced salt solution, non-essential amino acids, 1 mmol/L sodium pyruvate, 2 mmol/L L-glutamine, 1500 mg sodium bicarbonate/L) (ATCC, Manassas, VA, USA) supplemented with 10% FBS and 1% v/v penicillin/streptomycin (Invitrogen Corp.). Cells were plated in 24-well plates at a seeding density of 1.0×10^6 cells per well. Twenty-four hours after plating, cells were transfected as follows: (pgPXR-WT or hPXR,[30] or pgFXR-WT or hFXR expression plasmid[31]) (250 ng/well), pRL-tk control plasmid (5 ng/well) and (XREM-3A4-tk-luciferase reporter plasmid for PXR[32] or IR-1-tk-luciferase reporter plasmid for FXR[31]) (250 ng/well), using Lipofectamine 2000 (Invitrogen Corp.) following the manufacturer's instructions. Twenty-four hours after transfection, cells were treated with the ligands of interest. The endogenous ligands used were: dehydroepiandrosterone (DHEA), dehydroepiandrosterone sulfate (DHEA-S), testosterone, 5α-dihydrotestosterone (DHT), 5β-DHT, pregnenolone, progesterone, estrone (E1), estrone sulfate (E1S), β-estradiol (E2), 5α-androst-16-en-3-one (androstenone), 16,(5α)-androsten-3α-ol (3α-androstenol), 16,(5α)-androsten-3β-ol (3β-androstenol), 5,16-androstadien-3β-ol (androstadienol), 4,16-androstadien-3-one (androstadienone) (all from Steraloids, Inc, Newport, RI, USA), 3-methylindole (3MI, skatole), indole-3-carbinol, 3-methyloxindole, 3-hydroxy-3-methyloxindole (3HMOI) and lithocholic acid (LCA) (Sigma-Aldrich Inc, St Louis, MO, USA). Specific activators for PXR and FXR, based on studies in other species, were also used. For PXR, the known activators used were rifampicin and 5-pregnen-3β-ol-20-one-16α-carbonitrile (PCN) (Sigma-Aldrich Inc). For FXR, the known activators used were chenodeoxycholic acid (CDCA) and 3-(2,6-dichloro phenyl)-4-(3′-carboxy-2-chlorostilben-4-yl)oxymethyl-5-iso propylisoxazole (GW4064) (Sigma-Aldrich Inc). Stocks of all ligands, except for LCA and CDCA, were made at 20 mmol/L in dimethylsulfoxide (DMSO), and then diluted to a final concentration of 10 μmol/L in culture media. LCA and CDCA stocks were made at 200 mmol/L in DMSO, and then diluted to 100 μmol/L in culture media. A DMSO control treatment was also used, with DMSO at 0.05% (v/v) in culture media. Twenty-four hours after ligand treatment, the media was removed, cells were washed in 1× PBS, and cells were lysed following the Dual-Luciferase Assay protocol (Promega, Madison, WI, USA). The dual-luciferase assay was carried out following the manufacturer's instructions using a Sirius single tube luminometer with dual injectors (Berthold Detection Systems, Oak Ridge, TN, USA).

Potential antagonistic effects of the ligands of interest were also studied for pgPXR-WT and pgFXR-WT. This was done by plating and transfecting HepG2 cells as has already been described. Twenty-four hours after transfection, all cells transfected with pgPXR-WT were co-incubated with 10 μmol/L rifampicin along with 10 μmol/L of the ligands of interest. For the rifampicin control, cells were treated with 10 μmol/L rifampicin and 0.05% DMSO (v/v). For pgFXR-WT-transfected cells, all cells were treated with 100 μmol/L CDCA along with the ligands of interest, which were all at a concentration of 10 μmol/L. For the CDCA control, cells were treated with 100 μmol/L CDCA and 0.05% DMSO (v/v). Twenty-four hours after transfection, cells were lysed and the dual-luciferase assay carried out.

Due to the initial decrease in the activity of pgPXR and pgFXR seen with 10 μmol/L skatole treatment, further concentrations of skatole were used to determine the dose

Table 1 Realtime PCR primers

Target	Forward	Reverse
Total pgPXR	5′ ctccgcaagtgtctggaaag 3′	5′ attgtccgctgctcttcagt 3′
pgPXR-SV1	5′ atggcgggaggagaggag 3′	5′ ggcataggctggaagggtaa 3′
pgPXR-SV2	5′ tggtagcgtctggaactacaaacc 3′	5′ tggaagccacctgaagtaggaga 3′
pgPXR-SV3	5′ gccaaagtcatctcctacttcag 3′	5′ caggaacaggaatctggagaga 3′
pgPXR-SV4	5′ ggaagatggtagcgtctgga 3′	5′ tgggcataggctgaagtagga 3′
pgPXR-SV5		5′ gggcggtctgaagtagga 3′
Total pgFXR	5′ tatgaactcaggcgaatgcctgct 3′	5′ atccagatgctctgtctccgcaaa 3′
pgFXR-SV1	5′ ggaatgttggctgaatgtatgtat 3′*	5′ gttcagttttctccctgcaagac 3′
pgFXR-SV2	5′ gttggctgaatgcttgttaactg 3′	5′ gggtgagttcagttttctcctac 3′
pgFXR-SV3	5′ ggaatgttggctgaatgtatgtat 3′*	5′ gggtgagttcagttttctccct 3′
pgFXR-SV4	5′ agtcttgcaggttaaaggaaga 3′	5′ cagcaaagcaatctgatcttcgtgg 3′
pgFXR-SV5	5′ ggaatgttggctgaatgtatgtat 3′*	5′ tcttcctttaacctgcaagacttag 3′
β-Actin	5′ gacatccgcaaggacctcta 3′	5′ gaggcgcgatgatcttga 3′

Realtime primers used to determine expression levels of each pgPXR and pgFXR splice variants. Common primers between variants are denoted by (*)

dependence of its inhibitory effect. This was also done for hPXR and hFXR. Cells were transfected with either the human or pig ortholog of either PXR or FXR as has been previously described. Twenty-four hours after treatment, cells were treated with either 10 μmol/L rifampicin or 100 μmol/L CDCA along with skatole at 10, 5, 2.5, 1, 0.5 or 0.25 μmol/L concentrations. Twenty-four hours after treatment, cells were lysed and the dual-luciferase assay carried out.

Although the ligand complement of pgCAR has been determined previously,[26] the effect of skatole on pgCAR was not tested at that time. Due to the inverse agonist effect found for skatole on the transactivation of pgPXR and pgFXR, we determined the effect of skatole on the constitutive transactivation of pgCAR and hCAR. HepG2 cells were plated and cultured as has been described. Twenty-four hours after plating, cells were transfected as follows: pgCAR-WT[26] (250 ng/well), pRL-tk control plasmid (5 ng/well) and (NR1)$_5$-LUC luciferase reporter plasmid[33] (250 ng/well) using Lipofectamine 2000. Twenty-four hours after transfection, cells were treated with 0.05% DMSO (v/v) or skatole at 10, 5, 2.5, 1, 0.5 or 0.25 μmol/L concentrations. Twenty-four hours after treatment, cells were lysed and the dual-luciferase assay carried out.

Effects of pgPXR and pgFXR splice variants on transactivation

Each of the five pgPXR and five pgFXR splice variants were tested for transactivation of the reporter. HepG2 cells were plated as has been previously described. Twenty-four hours after plating, cells were transfected as follows: pgPXR (SV1 through SV5, except SV3) or pgFXR (SV1 through SV5) (250 ng/well), pRL-tk control plasmid (5 ng/well) and XREM-3A4-tk-luciferase reporter plasmid for PXR or IR-1-tk-luciferase reporter plasmid for FXR (250 ng/well), using Lipofectamine 2000 (Invitrogen Corp.) following the manufacturer's instructions. pgPXR-SV3 was not used because it encodes the same protein as pgPXR-SV2. Twenty-four hours after transfections, cells transfected with a pgPXR splice variant were treated with 10 μmol/L rifampicin and cells transfected with a pgFXR splice variant were treated with 100 μmol/L CDCA.

Twenty-four hours after treatment, cells were lysed and the dual-luciferase assay carried out.

To test for potential effects of the splice variants on the transactivation of the reporter by the wild-type receptor, plasmids for pgPXR-WT or pgFXR-WT were co-transfected with their respective splice variants, with each splice variant being co-transfected on an individual basis. Plates were seeded with HepG2 cells as described previously and 24 h after plating, cells were transfected as follows: pgPXR-WT or pgFXR-WT (125 ng/well), XREM-3A4-tk-luciferase reporter plasmid for PXR or IR-1-tk-luciferase reporter plasmid for FXR (250 ng/well), pRL-tk (5 ng/well), pgPXR splice variant or pgFXR splice variant (6.25, 3.13, 1.25 or 0.63 ng/well) and pcDNA 3.1 empty vector for a total amount of 500 ng plasmid/well, using Lipofectamine 2000 as a transfection reagent. Twenty-four hours after transfection, cells transfected with pgPXR-WT and its splice variants were treated with 10 μmol/L rifampicin, while cells transfected with pgFXR-WT and its splice variants were treated with 100 μmol/L CDCA. Twenty-four hours after treatment, cells were lysed and the dual-luciferase assay carried out.

Due to a sharp increase in transactivation with the co-transfection of pgFXR-WT and pgFXR-SV1, as well as with pgPXR-WT and pgPXR-SV1, further pgFXR-SV1 and pgPXR-SV1 inclusion levels were tested to determine whether these increases in the transactivation were dose dependent. Cells were plated and transfected as was described for the initial splice variant co-transfections, with pgFXR-SV1 or pgPXR-SV1 being included at 0.75, 0.875, 1.0 or 1.125 ng/well. Cells were treated with 0.05% v/v DMSO or 100 μmol/L CDCA for pgFXR-SV1 co-transfected cells and 0.05% v/v DMSO or 10 μmol/L rifampicin for pgPXR-SV1 co-transfected cells at 24 h after transfection. Twenty-four hours after ligand treatment, cells were lysed and the dual-luciferase assay carried out.

The effect of pgFXR-SV1 was also tested using hFXR to determine whether the dominant-positive effect seen was specific to pgFXR-WT. HepG2 cells were plated as described, then transfected as was done for the initial characterization of the pgFXR splice variants, but with pgFXR-WT replaced by hFXR for the transfections. Twenty-four hours after transfection, cells were treated

with 100 μmol/L CDCA, and then the dual-luciferase assay was carried out 24 h after treatment. To further ensure that the dominant-positive effect seen was not due to the individual activities of the splice variants, they were transfected into cells at their inclusion levels used for the dominant effect tests, but without a wild-type vector included. Cells were plated, then transfected 24 h after as described above, with empty vector (pcDNA 3.1) in place of any wild-type vector. Treatment and the luciferase assay were carried out as described above.

The effects of all splice variants together on the transactivation of the wild-type receptors were also tested. Cells were plated as described, and transfected as follows: for pgPXR (SV1 at 3.13 ng/well, SV2/3 at 3.13 ng/well, SV4 at 2.5 ng/well, SV5 at 2.5 ng/well and pgPXR-WT at 125 ng/well); for pgFXR (SV1 at 3.13 ng/well, SV2 at 4.375 ng/well, SV3 at 2.5 ng/well, SV4 at 1.25 ng/well, SV5 at 1.25 ng/well, and pgFXR-WT at 125 ng/well). Twenty-four hours after transfection, cells were treated with 10 μmol/L rifampicin (pgPXR-transfected cells) or 100 μmol/L CDCA (pgFXR-transfected cells) and 0.05% v/v DMSO or 10 μmol/L skatole. Cell lysing and the dual-luciferase assay were carried out as described.

The effects of pgPXR-SV1 and pgFXR-SV1 on skatole inhibition of the wild-type receptors were also tested. Cells were plated and transfected as already described, with pgPXR-SV1 or pgFXR-SV1 transfected at 0.00, 0.63, 0.875, 1.0, 1.125, 1.25 or 3.13 ng/well along with their corresponding wild-type receptor (125 ng/well) and reporter (250 ng/well). Twenty-four hours after transfection, pgPXR-SV1-transfected cells were treated with 10 μmol/L rifampicin and 10 μmol/L skatole while pgFXR-SV1-transfected cells were treated with 100 μmol/L CDCA and 0.05% v/v DMSO or 10 μmol/L skatole. Twenty-four hours after treatment, cells were lysed and the dual-luciferase assay carried out as already described.

Statistical analysis

Data on the effect of ligand treatment on transactivation of pig and human PXR and FXR were analysed with the Statistical Analysis System, version 9.1 (SAS Institute, Cary, NC, USA). Differences between treatment groups comparing ligand treatments with the DMSO vehicle control, and the effects of the pgPXR or pgFXR splice variants on the transactivation of wild-type pgPXR or pgFXR receptors were analyzed by the General Linear Model procedure followed by Dunnett's T-test and linear regression analysis to test for dose–response relationships. Differences between ortholog responses to ligands for PXR and FXR in pigs and humans were analyzed using the General Linear Model and paired *t*-tests comparing fold activation above the DMSO control.

Results

Cloning of pgPXR and pgFXR and their splice variants

The cloning and sequencing of pgPXR previously described[17] resulted in the isolation of five alternatively spliced variants. These variants were subcloned into the pcDNA3.1/V5-His TOPO vector to allow for expression studies to be carried out. These different variants had a variety of insertions and deletions, resulting in frameshift mutations and truncated proteins, which are further described in Pollock *et al.*[17]

Cloning of pgFXR-WT was initiated by generating an expected porcine sequence using pig ESTs aligned to the hFXR nucleotide sequence (gi:142360165). The resulting 1487 bp sequence was 91% homologous to the human sequence, and the expected 482 amino acid protein was 93% homologous to the human protein (Figure 1). There were no alterations between hFXR and pgFXR-WT in residues indicated as being important for ligand binding in hFXR.[34] PCR amplification of pgFXR from cDNA samples and subsequent cloning isolated the expected product, along with five alternatively spliced variants (Figure 2a). The coding regions of each variant had various additions or deletions at exon/exon boundaries, as judged from the human *FXR* gene structure, which resulted in alternative protein products (Figure 2b). pgFXR-SV1 has a 12 bp insertion between exons 5 and 6, which results in the addition of four amino acids (MYTG) to the DBD without shifting the reading frame, and this results in a protein of 486 amino acids. pgFXR-SV2 contained an additional 5 bp between exons 6 and 7, as well as a 38 bp deletion from the 3′ end of exon 7. This results in a loss of 11 amino acids within the hinge region of the protein, resulting in a protein of 471 amino acids. The third splice variant, pgFXR-SV3, contains the same deletion as pgFXR-SV2, as well as the 12 bp insertion seen in pgFXR-SV1. However, this variant does not contain the 5 bp insertion seen in pgFXR-SV2. As such there is a frameshift that results in a truncated protein that is 322 amino acids in length. Both pgFXR-SV4 and pgFXR-SV5 contain a deletion of the complete exon 7 (99 bp), with pgFXR-SV5 differing from pgFXR-SV4 by the addition of the 12 bp insertion seen in pgFXR-SV1. This results in 33 amino acid deletions from the hinge regions of each expected product of pgFXR-SV4 and pgFXR-SV5, which are 449 and 454 amino acids, respectively.

Determination of splice variant expression by realtime PCR

Realtime PCR was used to determine the mRNA expression levels of all pgPXR and pgFXR splice variants in the liver of 10 individual animals. Primers specific to each variant were designed across unique splice sites for each variant, as shown for pgPXR variants in Table 2 and for pgFXR variants in Table 3. Total mRNA levels for each nuclear receptor were determined by designing primers over conserved regions found in all splice variants. The relative levels of each variant of pgPXR and pgFXR were determined by calculating $\Delta\Delta$CT values, using β-actin as an internal control. The expression of each variant was then calculated as a percentage of the total amount of its respective nuclear receptor. This was done by expressing the $\Delta\Delta$CT for each variant as a percentage of the $\Delta\Delta$CT for the total nuclear receptor expressed.
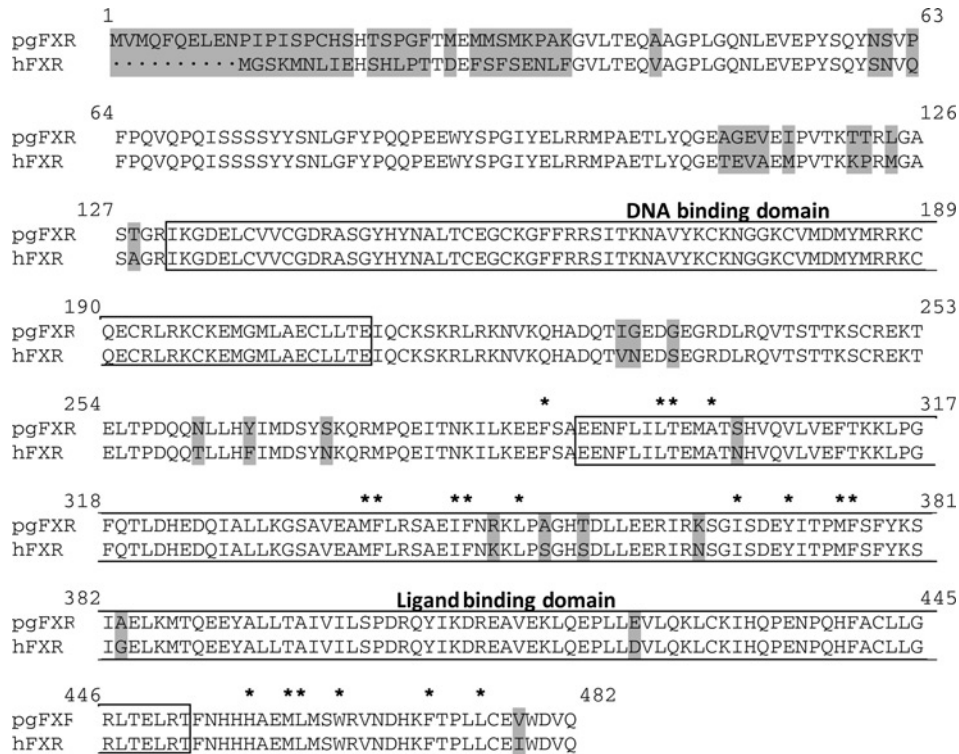
Figure 1 Protein alignment between pgFXR (pgFXR-WT) and hFXR. Amino acid changes between the orthologs are highlighted in grey. The DNA binding domains and ligand binding domains are denoted by boxes. Key ligand binding residues for hFXR are noted by (*)

The expression levels of each pgPXR splice variant with respect to total pgPXR are given in Table 4. pgPXR-SV5 was the most prevalent alternatively spliced variant on average, with a mean expression level of 1.51% in the 10 pigs, ranging from 1.15% to 1.86%. The highest expression of any single splice variant was pgPXR-SV1, which reached 2.49% of total pgPXR in a single individual. However, this variant had a mean expression level of 1.25%, due to large variation in expression levels between individual animals. The average expression levels of the other pgPXR splice variants ranged from 0.70% to 0.97%, with levels in individuals ranging from 0.17% to 1.83%. The alternatively spliced variants of pgPXR comprised 5.33% of the total pgPXR on average, with levels of individual splice variants ranging from 3.33% to 7.92%.

The expression levels of pgFXR splice variants were highly variable among individuals (Table 4). The most prevalent pgFXR alternative splice variant was pgFXR-SV2, which was present at a mean level of 2.34%, and ranged from 0.97% to 3.39% in individual pigs. The other variants had mean expression levels ranging from 0.41% (pgFXR-SV4) to 1.38% (pgFXR-SV1), and individual levels ranging from 0.03% to 2.19%. On average, pgFXR-SV1 through pgFXR-SV5 comprised 6.01% of total pgFXR, although individual levels ranged from 1.92% to 9.26%. The upper level of this range could potentially be enough to reduce overall pgFXR transactivation of the reporter by decreasing the expression of the wild-type receptor.

Tissue distribution of pgFXR

Porcine FXR was first isolated as part of this work, and as such the tissue distribution for this receptor in seven tissues (liver, small intestine, lung, heart, adrenal glands, kidney and testes) was measured. The relative levels of total pgFXR are given in Figure 3, with each tissue expression level presented relative to the liver expression level. pgFXR was expressed at high levels in all tissues, with the highest expression in the liver and the lowest expression in the testes.

Effects of ligands on the transactivation of human and pig PXR and FXR

Dual-luciferase reporter assays were used to determine the effect of different ligands on the transactivation of pig and human orthologs of PXR and FXR. For both hPXR and pgPXR-WT, 13 ligands significantly increased transactivation levels above that seen with the DMSO control; 12 of these ligands were shared by the two orthologs (Figure 4). Both orthologs of PXR responded significantly to the known hPXR activator rifampicin, with a 22.3-fold increase over DMSO control seen with pgPXR-WT and an 8.1-fold increase for hPXR. 5β-DHT and 5α-DHT, major metabolites of testosterone, were also active ligands for both pgPXR-WT (pg) and hPXR (h), increasing transactivation over DMSO control by (3.9 pg, 6.5 h)-fold and (3.2 pg, 4.6 h)-fold, respectively. Other ligands that activated both pgPXR-WT
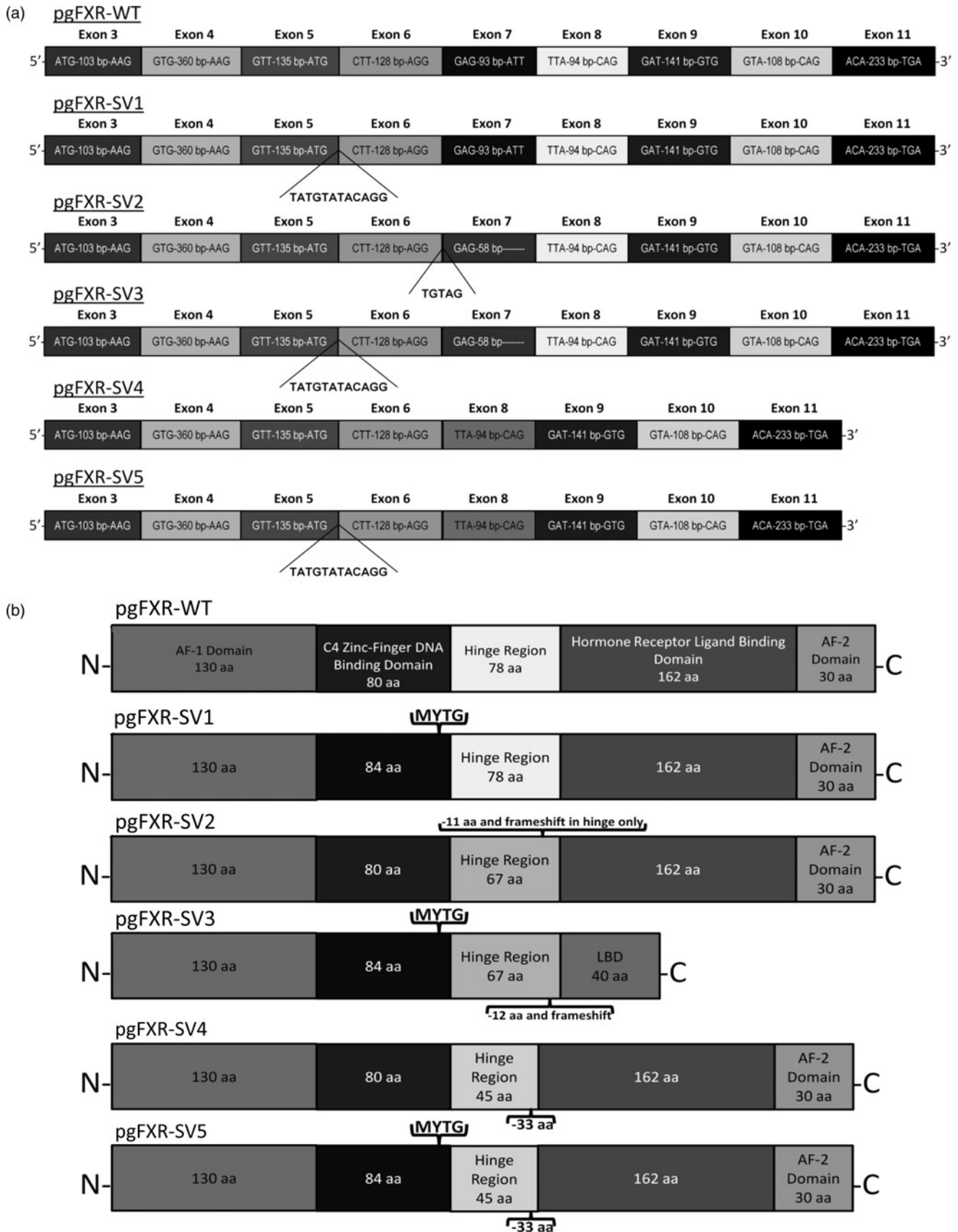
Figure 2 (a) Schematic diagram representing alternative splicing and exon junctions of pgFXR. Splice variants pgFXR-SV1, SV2, SV3 and SV5 have insert sequences at exon junctions that were determined by comparison with the cDNA and genomic sequences of hFXR. (b) Schematic diagram representing the deduced protein domain structure for the pgFXR splice variants

Table 2 Nucleotide alignment of pgPXR splice variants

Splice variant	Base	Sequence alignment
pgPXR-WT	1	ATGCAATGCAATGAAACAGACTCCACTTCTGGAAATTCCACCACCAATGCAGATGAGGAAGATGAGGGTCCCCAGAT
	78	CTGCCGTGTATGTGGGGACAAGGCCACTGGTTATCATTTCAATGTTATGACATGTGAAGGATGCAAGGGCTTTTTCAGGA
	158	GGGCCATCAAACGCAATGCCCGGCCCCGGTGCCTCTTCCGGAAGGGCGCCTGCGAGATCACCCGGAAGACTCGGCGGCAG
		Total pgPXR-F
	238	TGCCAGGCCTGCCGCCTCCGCAAGTGTCTGGAAAGCGGCATGAGGAAGGAAATGATCATGTCAGATGCAGCTGTGGAGCA
		→→→→→→→→→→→→→→→
		Total pgPXR-R
	318	GAGGCGGGCCTTGATCAGGAGGAAGAAACGAGAACAGATCGGGGCTCAGCCCCCAGGAGCCAAGGGTCTCACTGAAGAGC
		←←←←←←←←←←
	398	AGCGGACAATGATCAGTGAGCTGATGAACGTTCAGATGAAAACCTTTGACACCACCTTCACACATTTCAAGAATTTTCGG
	478	TTACCAGAGGTGCTTAGCAGTAGCCTCGAGATTCCAGAGTGTCTGCAGACTCCGTCGTCAAGGGAAGAAGCTGCCAAGTG
		pgPXR-SV4,6-F pgPXR-SV2-F
	578	GAGCAAGCTCAGGGAAGATCTGTGCTCAGTGAAACTCTCTCTGCAGCTAAGGGGGGAAGATGGTAGCGTCTGGAACTACA
		→→→→→→→→→→→
	638	AACCCCCAGCAGACAACAGTGGGAAAGAGATCTTTTCCCTGCTGCCCCACATAGCTGACATGTCAACCTACATGTTCAAA
		→
pgPXR-WT,SV1	718	GGCATTATCAACTTTGCCAAAGTCATCTCCTACTTCAGGGACTTGCCCATTGAGGACCAGATCTCTCTGCTGAAGGGGGC
		pgPXR-SV3-F pgPXR-SV2-R
pgPXR-SV2,3		GGCATTATCAACTTTGCCAAAGTCATCTCCTACTTCAGG∷∷∷∷∷∷∷∷∷∷∷∷∷∷∷∷∷∷∷∷∷∷∷∷∷∷∷∷∷∷∷∷∷∷∷∷∷
		←←←←←←→→→→→
		pgPXR-SV5-R pgPXR-SV4-R
pgPXR-SV4,5		GGCATTATCAACTTTGCCAAAGTCATCTCCTACTTCAG∷∷∷∷∷∷∷∷∷∷∷∷∷∷∷∷∷∷∷∷∷∷∷∷∷∷∷∷∷∷∷∷∷∷∷∷∷∷
		←←←←←←
pgPXR-WT,SV1	798	CACCTTTGAGCTGTGCCAGCTGAGATTCAACACGGTGTTCAACGCAGAGACGGGGACCTGGGAGTGTGGTCGGCTGTCCT
pgPXR-SV2,3,4,5		∷∷∷
pgPXR-WT	878	ACAGCTTGGAAGACCCCTCAGGTG∷∷∷
pgPXR-SV1		**pgPXR-SV1-F**
		ACAGCTTGGAAGACCCCTCAGGTGCCCTGGCAGAGGGAGGGGAACAGCCATGGCGGGAGGAGAGGAGCCAGGTCAGGATG
		→→→→→→→→→→→→
pgPXR-SV2,3,4,5		∷∷∷
pgPXR-WT,SV2,3,4,5	958	∷∷∷
pgPXR-SV1		TGCACGTCCTGGGATTGCAGGGCAGAAGACTGGGCGATGGGAAAAGAGACCCTGGTGAGACAAGTCTGGGTGTTGGGTCA
pgPXR-WT		∷∷∷∷∷∷∷∷∷∷∷∷∷∷∷∷∷∷∷∷∷∷∷∷∷∷∷∷∷∷∷∷GCTTCCAGCAGCTTCTCCTGCAGCCCATGCTGAA
pgPXR-SV1		**pgPXR-SV1-R**
		GCTTCCTGAGGAGTTTACCCTTCCAGCCTATGCCCACCCACAGGTGGCTTCCAGCAGCTTCTCCTGCAGCCCATGCTGAA
		←←←←←←←←
		pgPXR-SV2-R
pgPXR-SV2,3	1038	∷∷∷∷∷∷∷∷∷∷∷∷∷∷∷∷∷∷∷∷∷∷∷∷∷∷∷∷∷∷∷∷∷∷∷∷∷TGGCTTCCAGCAGCTTCTCCTGCAGCCCATGCTGAA
		←←←←←←
		pgPXR-SV4-R
pgPXR-SV4		∷∷∷∷∷∷∷∷∷∷∷∷∷∷∷∷∷∷∷∷∷∷∷∷∷∷CCTATGCCCACAGGTGGCTTCCAGCAGCTTCTCCTGCAGCCCATGCTGAA
		←←←←←←
pgPXR-SV5		∷∷∷
		pgPXR-SV3-R
pgPXR-WT,SV1,2,3,4	1118	ATTCCACTACATGCTGAAGAAGCTGCAGCTGCATAAGGAGGAGTATGTGCTGATGCAGGCCATCTCCCTTTTCTCTCCAG
		←←←←←←
		pgPXR-SV5-R
pgPXR-SV5		∷∷∷
		←←←←←
		pgPXR-SV5-R
pgPXR-WT,SV1,2,4,5	1198	ACCGCCCGGGTGTGGTGCAACGCCAAGTGGTGGACCAGCTGCAGGAGAGGTTTGCCATTACCCTGAAGGCCTACATCGAG
		pgPXR-SV3-R
pgPXR-SV3		A∷∷
pgPXR-WT	1278	TGCAACCGGCCCCAGCCTGCCCACCGATTCCTGTTCCTGAAGATCATGGCTATGCTCACTGAGCTCCGCAGCATCAACGC
pgPXR-SV1		TGCAACCGGCCCCAGCCTGCCCACCGAT
aaPXR-SV2,4,5		TGCAACCGGCCCCAGCCTGCCCACCGATTCCTGTTCCTGAAGATCATGGCTATGCTCACTGAGCTCCGC
		pgPXR-SV3-R
pgPXR-SV3		∷∷∷∷∷∷∷∷∷∷∷∷∷∷∷∷∷∷∷TTCCTGTTCCTGAAGATCATGGCTATGCTCACTGAGCTCCGC
		←←←←←←
pgPXR-WT	1358	CCAACACACCCAGCGGCTGCTGCGAATCCAGGACATACACCCCTTCGCCACCCCACTCATGCAGGAGTTATTCAGCATCA
	1438	CAGAAAGCTGA

The consensus sequence and base numbers of the wild-type sequence of pgPXR (pgPXR-WT) are given, and aligned with the splice variants pgPXR-SV1 to pgPXR-SV5. Regions where the sequence of a splice variant differs from pgPXR-WT are shown. Realtime primers for each pgPXR variant, as well as total pgPXR, are depicted as colored boxes, with direction noted by an arrow. Areas where primers overlap are denoted by a lighter grey

Table 3 Nucleotide alignment of pgFXR splice variants

Splice variant	Base	Sequence alignment
pgFXR-WT	1	ATGGTAATGCAGTTTCAGGAGTTAGAAAATCCAATTCCAATCAGTCCTTGTCACAGCCACACGTCGCCTGGGTTTACCAT
	81	GGAGATGATGAGCATGAAGCCTGCCAAAGGTGTACTAACAGAACAAGCAGCAGGTCCTCTGGGACAGAATCTCGAAGTGG
	161	AACCATACTCACAATACAACAGTGTTCCGTTTCCTCAAGTTCAACCACAGATTTCCTCATCTTCCTATTATTCCAACCTG
	241	GGTTTCTACCCCCAGCAGCCTGAAGAGTGGTACTCTCCTGGCATA**TATGAACTCAGGCGAATGCCTGCT**GAGACTCTCTA *Total pgFXR-F*
	321	CCAGGGAGAGGCTGGGGAAGTAGAGATTCCTGTGACAAAGACGACCCGACTGGGTGCATCAACAGGGAGAATAAAAGGGG
	401	ATGAGCTTTGTGTCG**TTTGCGGAGACAGAGCATCTGGAT**ACCATTATAATGCACTGACCTGTGAGGGGTGCAAAGGTTTC *Total pgFXR-F*
	481	TTCCGGAGAAGCATTACCAAACATGCGAAGGAAGTGCCAGGAGTGTCGACTAAGGAAATGCAAAGAGATGACATGCGAAG
pgFXR-WT,SV2,4	561	GAAGTGCCAGGAGTGTCGACTAAGGAAATGCAAAGAGATGGGAAT**GTTGGCTGAATG**::::::::::::**CTTGTTAACTG** *pgFXR-SV2-F*
pgFXR-SV1,3,5		GAAGTGCCAGGAGTGTCGACTAAGGAAATGCAAAGAGATG**GGAATGTTGGCTGAATGTATGTAT**ACAGGCTTGTTAACTG *pgFXR-SV1,4,6-F*
pgFXR-WT	641	AAATTCAGTGTAAATCTAAACGACTGAGAAAAAACGTGAAGCAGCATGCAGATCAGACCATTGGTGAAGACGGCGAAGGA
pgFXR-WT,SV1,3	721	CGTGACTTGCGACAAGTGACCTCAACAACTAA**GTCTTGCAGG**::::::**GAGAAAACTGAACTCACCC**CAGATCAACAGAAT *pgFXR-SV1-R* *pgFXR-SV3-R*
pgFXR-SV2		CGTGACTTGCGACAAGTGACCTCAACAACTAAGTCTTGCAGGT**GTAGGAGAAAACTGAACTCACCC**CAGATCAACAGAAT *pgFXR-SV2-R*
pgFXR-SV4,5		CGTGACTTGCGACAAGTGACCTCAACAA**CTAAGTCTTGCAGG**::::::::::::::::::::::::::::::::::::::: *pgFXR-SV5-R* *pgFXR-SV4-F*
pgFXR-WT,SV1	801	CTTCTTCATTATATTATGGATTCATATAGTAAGCAGAGGATGCCTCAGGAAATAACAAATAAAATTTTAAAGGAAGAATT
pgFXR-SV2,3		CTTCTTCATTATATTATGGATTCATATA::TTAAAGGAAGAATT
pgFXR-SV4,5		:::**::**::::::::::::**TTAAAGGAAGA**ATT *pgFXR-SV5-R* *pgFXR-SV4-F*
pgFXR-WT	881	CAGTGCAGAAGAAAATTTTCTCATTTTAACGGAAATGGCTACCAGTCATGTACAGGTCCTCGTAGAATTCACAAAAAAAC
	961	TTCCAGGATTTCAGACATTGGA**CCACGAAGATCAGATTGCTTTGCTG**AAAGGATCTGCAGTTGAAGCTATGTTTCTCCGT *pgFXR-SV4-R*
	1041	TCAGCTGAGATTTTCAATAGGAAACTTCCGGCTGGACATACTGACCTATTGGAAGAAAGAATTCGAAAGAGTGGTATCTC
	1121	CGATGAATATATAACACCTATGTTCAGTTTTTATAAAAGTATTGCTGAATTAAAAATGACTCAAGAAGAATACGCTCTGC
	1201	TTACAGCAATTGTTATCCTCTCTCCAGACAGACAATACATAAAGGACCGAGAGGCAGTAGAGAAGCTTCAGGAACCACTG
	1281	CTTGAGGTGCTACAAAAGTTGTGTAAGATTCATCAGCCTGAAAATCCTCAACATTTTGCCTGCCTCCTGGGTCGCCTGAC
	1361	TGAGTTGCGGACATTCAACCATCACCACGCAGAGATGCTTATGTCATGGAGAGTGAATGACCACAAGTTTACCCCGCTTC
	1441	TCTGTGAAGTCTGGGATGTGCAGTGA

The consensus sequence and base numbers of the wild-type sequence of pgFXR (pgFXR-WT) are given, and aligned with the splice variants pgFXR-SV1 to pgFXR-SV5. Regions where the sequence of a splice variant differs from pgFXR-WT are shown. Realtime primers for each pgFXR variant, as well as total pgFXR, are depicted as colored boxes, with direction noted by an arrow. Areas where primers overlap are denoted by a lighter grey

and hPXR were testosterone (2.9 pg, 2.9 h), progesterone (4.6 pg, 5.4 h), E1 (3.7 pg, 3.6 h), E1S (4.8 pg, 3.3 h), E2 (5.2 pg, 5.5 h), 3α-androstenol (3.4 pg, 2.4 h), androstadienone (6.4 pg, 3.5 h), 3HMOI (3.0 pg, 2.5 h) and LCA (12.2 pg, 4.6 h). pgPXR-WT also significantly responded to the known mouse PXR activator PCN, with a 5.3-fold increase in transactivation seen above the DMSO control. hPXR also responded significantly to DHEA (3.2-fold), while pgPXR-WT did not. Of the 22 ligands tested with the two PXR orthologs, eight generated responses in pgPXR-WT and hPXR that were not significantly different between the two orthologs. Six of these eight ligands were significant agonists shared by pgPXR-WT and hPXR, namely testosterone, progesterone, the estrogens (E1, E1S, E2) and 3α-androstenol.

A similar experiment was carried out using the porcine and human FXR orthologs, testing 22 ligands for their abilities to cause an increase in pgFXR-WT and hFXR activities above a DMSO control. Both orthologs significantly responded to three ligands, two of which were shared between pgFXR-WT and hFXR (Figure 5). CDCA, a bile acid and known hFXR agonist, significantly increased pgFXR-WT transactivation 11.0-fold and hFXR transactivation by 13.3-fold. The second known hFXR agonist tested, the synthetic ligand GW4064, also significantly increased pgFXR-WT and hFXR transactivation, by 9.2- and 21.0-fold, respectively. pgFXR significantly responded to progesterone, with a 2.1-fold increase in transactivation. The third agonist seen for hFXR was LCA, another bile acid and known hFXR agonist, which increased hFXR transactivation by 3.4-fold.

The chosen ligands were further tested to determine whether they would have any antagonistic effects on pgPXR-WT or pgFXR-WT. Cells transfected with each nuclear receptor were first treated with the agonist found to be most effective in increasing transactivation above the DMSO control. Thus, pgPXR-WT-transfected cells

Table 4 Amounts of individual and total pgPXR and pgFXR splice variants determined using realtime PCR

Receptor variant	Mean (%)	Lower limit (%)	Upper limit (%)
pgPXR-WT	94.66	92.08	96.67
pgPXR-SV1	1.25	0.17	2.49
pgPXR-SV2	0.70	0.51	1.53
pgPXR-SV3	0.90	0.71	1.16
pgPXR-SV4	0.97	0.69	1.83
pgPXR-SV5	1.51	1.15	1.86
Total (pgPXR-SV1 to 5)	5.33	3.33	7.92
pgFXR-WT	93.99	90.74	98.08
pgFXR-SV1	1.38	0.39	2.19
pgFXR-SV2	2.34	0.97	3.39
pgFXR-SV3	1.10	0.26	2.05
pgFXR-SV4	0.41	0.03	1.27
pgFXR-SV5	0.79	0.19	1.55
Total (pgFXR-SV1 to 5)	6.01	1.92	9.26

Each value is expressed as a percentage of total receptor transcripts

were initially treated with 10 μmol/L rifampicin and pgFXR-WT-transfected cells were treated with 100 μmol/L CDCA, and then treated with the other ligands. Of these, only skatole showed a significant antagonistic effect on the transactivation of both nuclear receptors. Skatole treatment at 10 μmol/L decreased the transactivation of the reporter by pgPXR-WT by $36.2 \pm 6\%$ below the transactivation level seen with just rifampicin treatment ($P = 0.05$; $n = 12$), while pgFXR-WT transactivation was decreased by skatole treatment at 10 μmol/L by $57.6 \pm 10\%$ ($P = 0.05$; $n = 12$) below the level seen with CDCA treatment. The constitutive transactivation of pgCAR-WT was also inhibited by skatole treatment at 10 μmol/L by $23.2 \pm 4\%$ ($P = 0.05$; $n = 12$) below the DMSO control.

The inhibition of pgPXR-WT, pgFXR-WT and pgCAR-WT by skatole was further investigated by determining if the effect was dose dependent, and if the effect was species specific. Further skatole concentrations (0.25, 0.5, 1, 2.5 and 5 μmol/L) were tested on the transactivation of both the pig and human orthologs of each receptor (Figure 6). Linear regression indicated that the inhibition by skatole on the transactivation of the human and pig orthologs for all three receptors was dose dependent ($P < 0.01$).
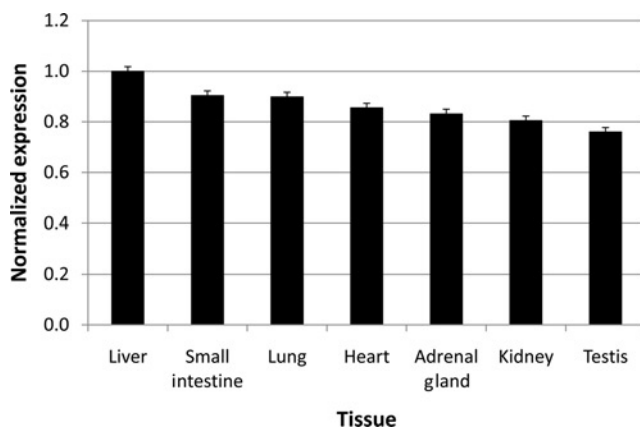
Figure 3 Expression of pgFXR mRNA in seven tissues. Levels of expression are presented relative to the expression seen in liver samples (mean $\pm$ SEM, $n = 4$)

Significant inhibition of pgPXR-WT and pgCAR-WT first occurred at the 1 μmol/L skatole treatment level (Figures 6b and c), while inhibition of their human orthologs first occurred at the 2.5 μmol/L treatment level. Significant inhibition of pgFXR-WT first occurred at the 5 μmol/L skatole treatment level, while significant inhibition of hFXR first occurred at the 0.25 μmol/L treatment level (Figure 6a).

Effects of pgPXR splice variants on pgPXR-WT transactivation

The transactivation activities of the pgPXR splice variants were tested using the dual-luciferase reporter assay for PXR. The transactivation activities of the five pgPXR splice variants, pgPXR-SV1 through pgPXR-SV5, were tested individually, as well as in a system co-expressing the splice variants with the wild-type, pgPXR-WT. This second system was employed to determine if any of the splice variants would affect the transactivation of wild-type pgPXR-WT. When transfected in the absence of pgPXR-WT and treated with rifampicin, none of the pgPXR splice variants significantly increased reporter response above that seen with pgPXR-WT treated with DMSO (data not shown). When co-expressed with pgPXR-WT, pgPXR-SV1 and pgPXR-SV2 significantly ($P = 0.05$) increased the transactivation of pgPXR-WT with rifampicin treatment (Figure 7a). Co-transfection of pgPXR-SV1 at 2.5% and 5.0% of the inclusion rate of pgPXR-WT significantly increased the transactivation by 62.3% and 53.8%, respectively, over what was found with pgPXR-WT alone. Co-transfection with pgPXR-SV2 also increased transactivation by 57.0% at the 5% inclusion level; however, this level is above the physiological range measured in this work. pgPXR-SV4 and pgPXR-SV5 showed no significant effect on pgPXR-WT transactivation.

Initial tests with co-transfection of pgPXR-SV1 along with pgPXR-WT resulted in sharp increases in pgPXR-WT transactivation between two of the tested inclusion levels; as such, additional 0.6%, 0.7%, 0.8% and 0.9% inclusion levels of this splice variant were tested to demonstrate that this effect was dose dependent (Figure 7b). Linear regression analysis showed that the increase in pgPXR-WT transactivation by pgPXR-SV1 inclusion was dose dependent ($P < 0.01$). The effect of pgPXR-SV1 on the transactivation of pgPXR-WT was then tested in the absence of an activating ligand. pgPXR-SV1 caused significant increases in pgPXR-WT transactivation at the 0.7%, 0.8%, 1.0% and 2.5% inclusion levels, with increases in the dual-luciferase ratios by 0.03, 0.04, 0.07 and 0.12, respectively (data not shown). These results suggest that pgPXR-SV1 confers some constitutive transactivation on pgPXR-WT.

The effect of all pgPXR splice variants combined on the transactivation of pgPXR-WT was tested, to determine if the dominant-positive effect of pgPXR-SV1 would still be present. Each variant was included at the highest percentage seen in the realtime PCR data. The inclusion of all splice variants resulted in an increase in pgPXR-WT activity by 54.5% ($\pm 8.6\%$), which was not significantly different ($P < 0.05$) than the increase of 62.1% ($\pm 13.6\%$) in pgPXR-WT transactivation obtained when just pgPXR-SV1 was co-transfected.
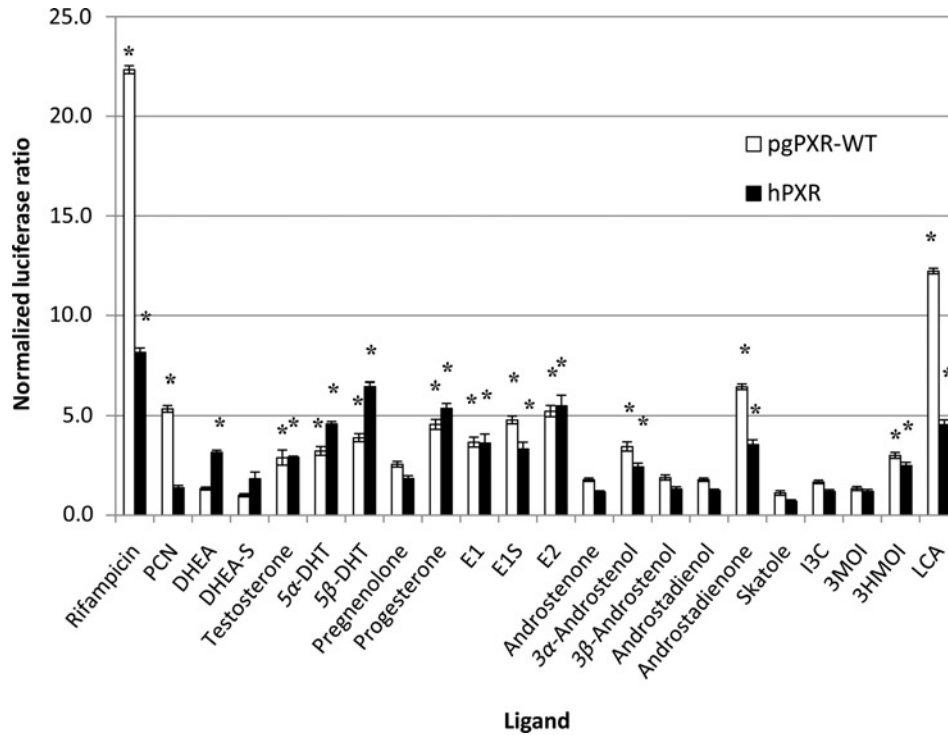
Figure 4   Response of pgPXR-WT (clear bars) and hPXR (colored bars) to tested ligands, in fold response above response to DMSO control, which was set to 1. Significant fold change ($P < 0.05$) compared with the control is denoted by (*). Ligands with a significant difference in fold response between pgPXR-WT and hPXR are denoted by (♦). Data from triplicates repeated four times (mean ± SEM). DMSO, dimethylsulfoxide; PCN, 5-pregnen-3β-ol-20-one-16α-carbonitrile; DHEA, dehydroepiandrosterone; DHEA-S, dehydroepiandrosterone sulfate; DHT, 5α-dihydrotestosterone; I3C, indole-3-carbinol; 3MOI, 3-methyloxindole; 3HMOI, 3-hydroxy-3-methyloxindole; LCA, lithocholic acid
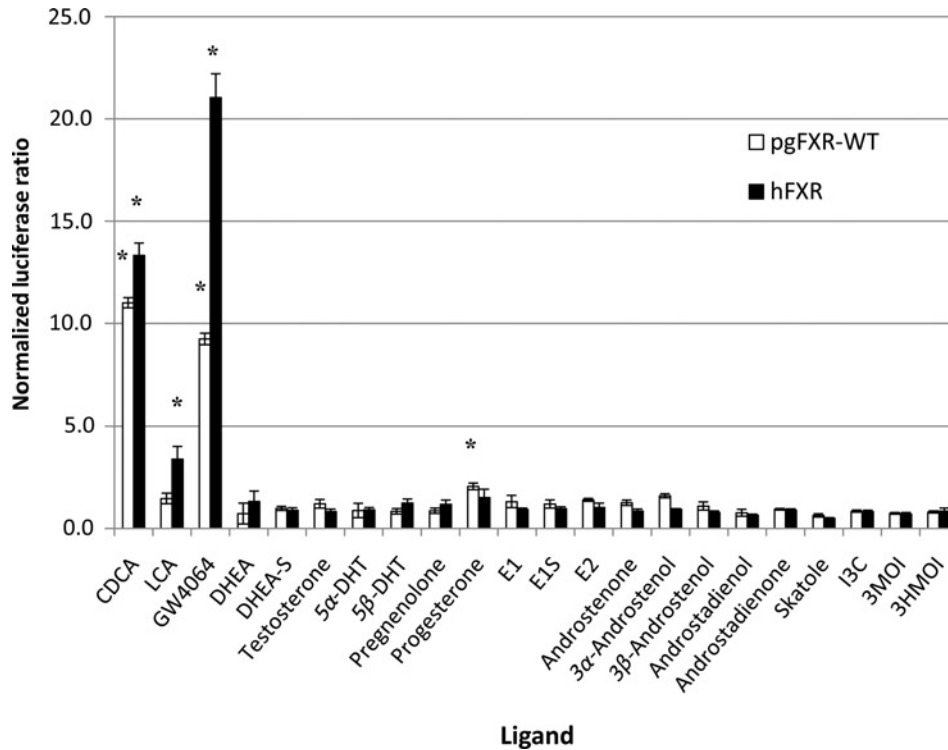
Figure 5   Response of pgFXR-WT (clear bars) and hFXR (colored bars) to tested ligands, in fold response above response to DMSO control, which was set to 1. Significant fold change ($P < 0.05$) compared with the control is denoted by (*). Ligands with a significant difference in fold response between pgFXR-WT and hFXR are denoted by (♦). Data from triplicates repeated four times (mean ± SEM). DMSO, dimethylsulfoxide; CDCA, chenodeoxycholic acid; DHEA, dehydroepiandrosterone; DHEA-S, dehydroepiandrosterone sulfate; DHT, 5α-dihydrotestosterone; I3C, indole-3-carbinol; 3MOI, 3-methyloxindole; 3HMOI, 3-hydroxy-3-methyloxindole; LCA, lithocholic acid
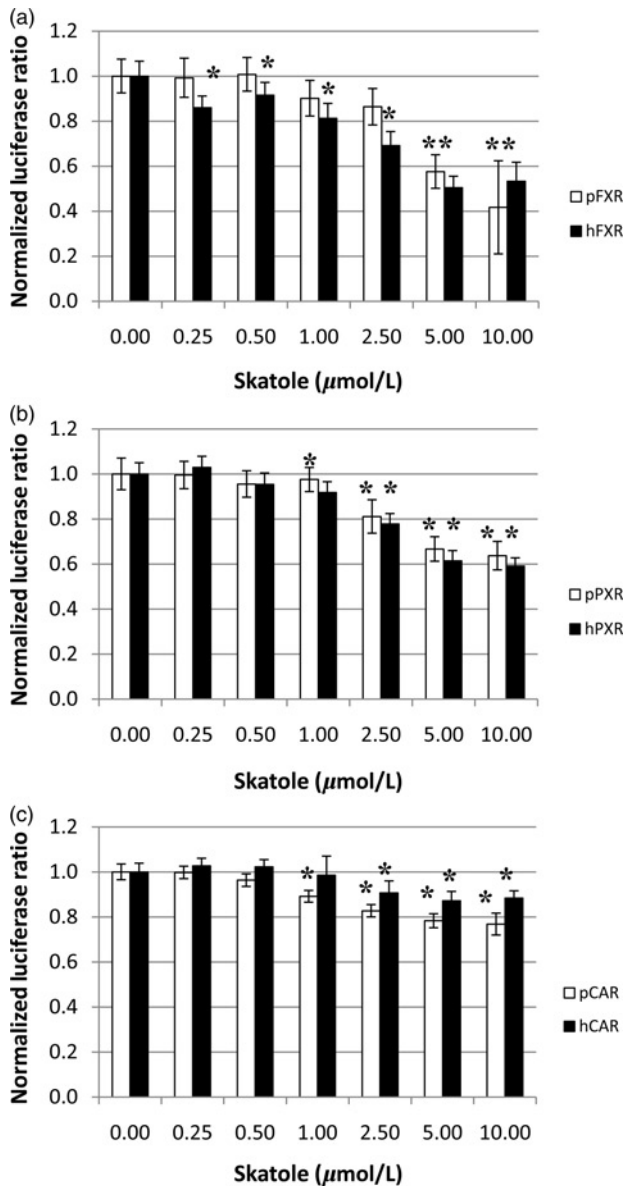
Figure 6 Effects of increasing concentrations of skatole on the transactivation activity of (a) pgFXR-WT (clear bars) and hFXR (colored bars), (b) pgPXR-WT (clear bars) and hPXR (colored bars) and (c) pgCAR-WT (clear bars) and hCAR (colored bars) normalized to the zero skatole treatment. Significant differences ($P < 0.05$) in normalized luciferase ratios compared with no skatole controls are indicated by (*). Data from triplicates repeated four times (mean $\pm$ SEM)

Effects of pgFXR splice variants on pgFXR-WT transactivation

The individual activities of the pgFXR splice variants, and their potential effects on the transactivation of pgFXR-WT, were tested using the dual-luciferase assay for FXR. Only pgFXR-SV1 showed any significant ($P = 0.05$) individual transactivation when treated with CDCA, with a 10.7-fold increase in transactivation compared with the pgFXR-WT-transfected DMSO-treated control (data not shown). This level of transactivation was not significantly different ($P > 0.05$) than the transactivation seen when an equivalent amount of pgFXR-WT was transfected. When pgFXR-SV1 was co-transfected with pgFXR-WT at inclusion

levels of 1.0%, 2.5% and 5.0%, the transactivation was increased by 75.5%, 90.2% and 81.6%, respectively (Figure 8a). Additional inclusion levels of pgFXR-SV1 were then tested to determine if the increase was dose dependent (Figure 8b). Inclusion of pgFXR-SV1 at 0.8% and 0.9% of the amount of pgFXR-WT resulted in significant increases of 80.6% and 86.9% compared with pgFXR-WT alone. Linear regression analysis indicated that the increase in transactivation was dose dependent ($P < 0.01$). The other pgFXR splice variants were not active individually (data not shown) and did not affect transactivation when co-transfected alongside pgFXR-WT (Figure 8a).

The effects of all pgFXR splice variants on the transactivation of pgFXR-WT were tested to determine if the non-effective variants would hinder the dominant-positive effect of pgFXR-SV1. Each variant was included at the highest percentage seen in the realtime PCR data. The inclusion of all splice variants resulted in an increase in pgFXR-WT transactivation by 88.8% ($\pm 2.9\%$). This increase in transactivation was not significantly different ($P < 0.05$) than the increase in pgFXR-WT transactivation of 90.0% ($\pm 3.8\%$) obtained when just pgfXR-SV1 was co-transfected at the 2.5% inclusion level.

The specificity of the pgFXR-SV1 dominant-positive effect was next tested by determining if the effect was found when pgFXR-WT was replaced by hFXR in co-transfection experiments. A significant increase in transactivation was seen at inclusion levels of 2.5%, 5% and 10% of pgFXR-SV1 (Figure 9), corresponding to increases in the dual-luciferase ratio of 0.13, 0.17 and 0.21, respectively. To determine if this increase was due to a dominant-positive effect or just the inclusion of the active pgFXR-SV1 variant, pgFXR-SV1 transactivation was tested at the same inclusion levels used but without the hFXR expression vector. The dual-luciferase ratios at 2.5%, 5% and 10% inclusion levels were 0.11, 0.14 and 0.20 higher than the DMSO controls (Figure 9). This indicates that the transactivation increase seen with pgFXR-SV1 co-transfection with hFXR was due to the individual transactivation of pgFXR-SV1 and not a dominant-positive effect. The effect of pgFXR-SV1 on pgFXR-WT was also tested in the absence of activating ligand to determine whether the transactivation increase seen was due to constitutive transactivation. There were significant increases in the dual-luciferase ratios of 0.03, 0.07 and 0.11 at inclusion levels of 0.8%, 1.0% and 2.5%, respectively (data not shown), indicating that pgFXR-SV1 may have conferred some constitutive transactivation on pgFXR-WT.

Effects of pgPXR-SV1 and pgFXR-SV1 on skatole inhibition

Due to the dominant-positive effects seen with pgPXR-SV1 and pgFXR-SV1, the effect of combining these splice variants with the inhibition of wild-type receptor activity caused by skatole was studied. It was found that both pgPXR-SV1 and pgFXR-SV1 were able to reverse the inhibitory effect of skatole on the corresponding wild-type receptor (Figure 10). pgPXR-SV1 reversed the inhibition significantly at the 0.9, 1.0 and 2.5% inclusion levels
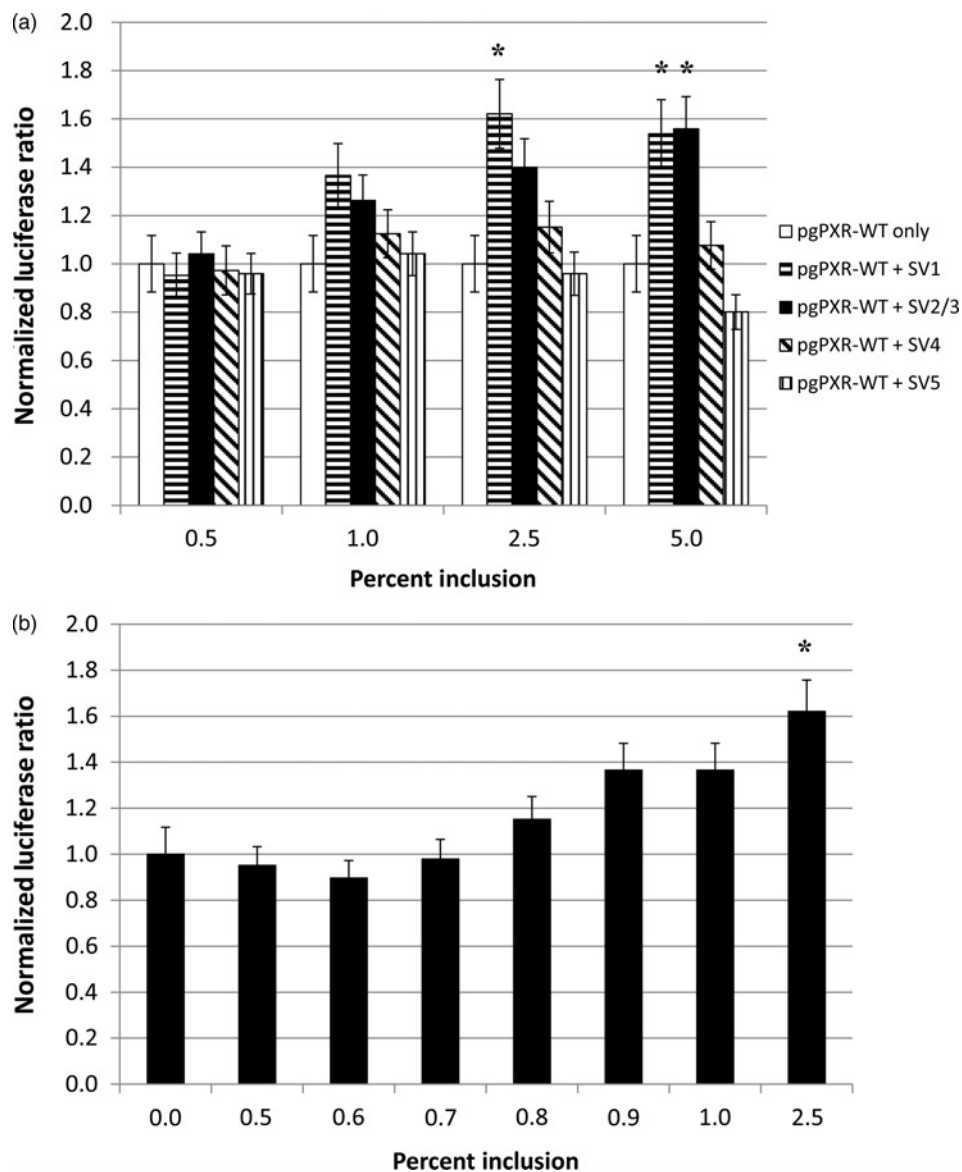
Figure 7 (a) Effects of co-transfection with pgPXR splice variants on transactivation of pgPXR-WT after rifampicin treatment. (b) Effect of co-transfection with low levels of inclusion (percentage of pgPXR-WT amount transfected) of pgPXR-SV1 on transactivation of pgPXR-WT with rifampicin treatment. Significant fold change ($P < 0.05$) compared with pgPXR-WT transactivation without splice variant inclusion is indicated by (*). Data from triplicates repeated four times (mean $\pm$ SEM)

(Figure 10a), while pgFXR-SV1 did so at the 0.8, 0.9, 1.0 and 2.5% inclusion levels (Figure 10b).

Discussion

The purpose of this work was to characterize the porcine orthologs of PXR and FXR, and compare their activities to their human counterparts. pgPXR-WT was previously cloned, along with five alternatively spliced variants, and its sequence compared with the hPXR sequence.[17] pgFXR-WT was cloned as part of this study using primers designed from a reference sequence assembled from pig ESTs with the human FXR as template. The sequence that was isolated from porcine liver cDNA was 91% homologous to the hFXR coding sequence from exon 4 through exon 11,

while only 81% homologous in exon 3. The resulting pre-dicted protein product is 93% homologous to hFXR from amino acid 37 onwards, with the first 36 amino acids retaining only 77% homology due to the divergence in the exon 3 sequence. The LBD contained no differences within key ligand binding residues identified for hFXR.[34]

This paper is the first report of pgFXR being cloned, and as such expression levels for this receptor were measured in seven tissues. pgPXR had been previously cloned and expression levels for several tissues were determined.[17] It was found that the liver expressed pgFXR at the highest level, while the testes expressed it at the lowest level, which was approximately 80% of the level seen in the liver. This expression range is similar to that seen in humans as shown using the BioGPS program,[35] which employed microarray data from Su *et al.*[36] As is shown in
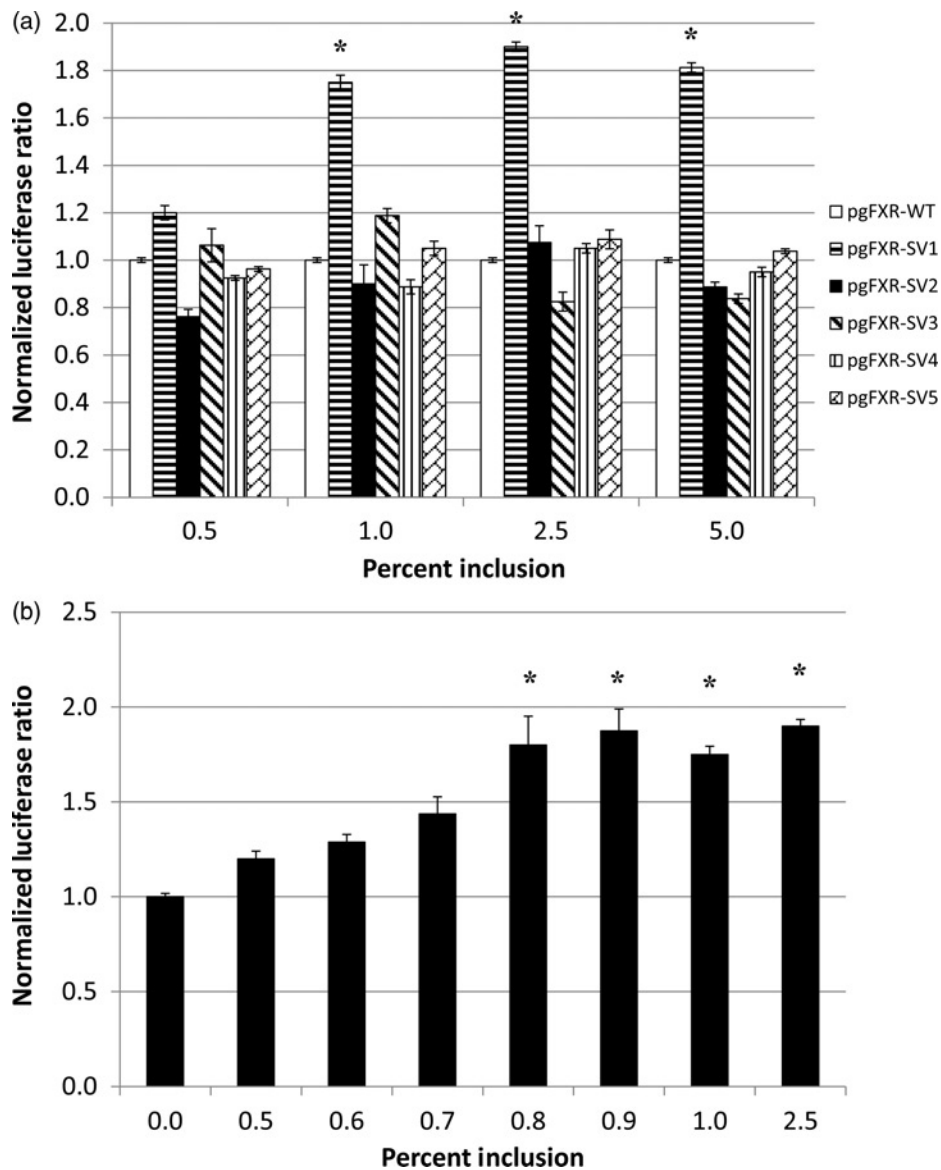
Figure 8 (a) Effects of co-transfection with pgFXR splice variants on transactivation of pgFXR-WT after CDCA treatment. (b) Effect of low percentages of inclusion (percentage of pgFXR-WT amount included) of pgFXR-SV1 on transactivation of pgFXR-WT after CDCA treatment. Significant fold change ($P <$ 0.05) compared with pgFXR-WT transactivation without splice variant inclusion is indicated by (*). Data from triplicates repeated four times (mean $\pm$ SEM). CDCA, chenodeoxycholic acid

the pig in this study, FXR is ubiquitously expressed in human tissues in a very narrow range of expression levels.

During the course of pgFXR-WT cloning, five alternatively spliced variants were also isolated (pgFXR-SV1 through pgFXR-SV5). Three of these variants, pgFXR-SV1, pgFXR-SV3 and pgFXR-SV5, contained a four amino acid (MYTG) insert at the C-terminal end of the DBD. This insertion has also been found in an alternatively spliced variant of hFXR that results in a decrease in transactivation,[37] likely due to altered protein folding. pgFXR-SV3 also had a 38 bp deleted from the 3′ end of exon 7, which results in a frameshift in the coding sequence and a truncated protein product. This product would not be expected to be able to act as a viable transcription factor, due to the loss of the AF-2 domain, which is required for ligand-dependent transactivation,[1] as well as the majority of the

LBD. The variants 2, 4 and 5 had deletions within the hinge region only, which may alter protein transactivation through altered protein folding. Variant 1 contained only the MYTG insert.

The expression levels of each of the pgPXR and pgFXR splice variants were determined using realtime PCR. pgPXR-SV5 was the most prevalent splice variant of pgPXR, with an average of 1.5% of total pgPXR, although pgPXR-SV1 had the highest expression level in a single individual at 2.5% of total pgPXR. The average amount of total alternatively spliced variants of pgPXR was 5.3%, with individual variation ranging from 3.3% to 7.9%. The profile of pgFXR splice variants was far more variable between individuals than the expression of pgPXR variants. On average, pgFXR-SV2 was the most prevalent variant at 2.3%, while pgFXR-SV4 was the least prevalent at 0.4% of
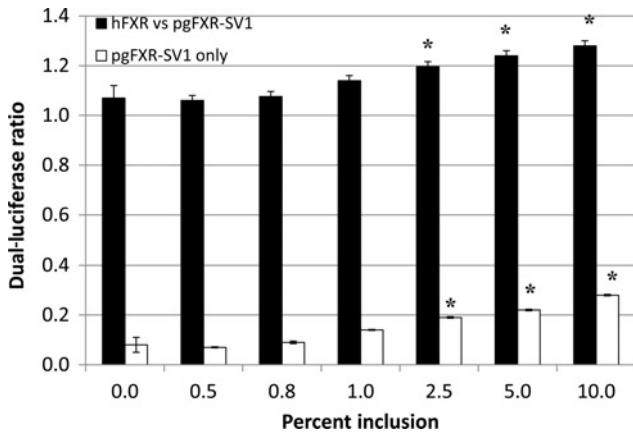
Figure 9 Effect of co-transfection with pgFXR-SV1 on hFXR transactivation (dark bars) and transactivation of pgFXR-SV1 in the absence of a wild-type receptor (light bars) after CDCA treatment. Significant fold change ($P < 0.05$) compared with controls without pgFXR-SV1inclusion indicated by (*). Data from triplicates repeated four times (mean $\pm$ SEM). CDCA, chenodeoxycholic acid

total pgFXR. These two variants also had the highest and lowest individual levels seen, with pgFXR-SV2 reaching 3.4% of total pgFXR in a single individual, while pgFXR-SV4 was as low as 0.03% in another individual. There was a large degree of variation seen in the percentage

Figure 10 (a) Effects of pgPXR-SV1 on transactivation of pgPXR-WT in the presence of 10 μmol/L skatole. (b) Effects of pgFXR-SV1 on transactivation of pgFXR-WT in the presence of 10 μmol/L skatole. Significant fold change ($P < 0.05$) compared with controls without splice variant inclusion indicated by (*). Data from triplicates repeated four times (mean $\pm$ SEM)

of total pgFXR that was comprised of splice variants, with an average of 6.0% with upper and lower limits of 9.3% and 1.9%, respectively. Although each variant protein would be expected to have altered or abolished transactivation, and as such may play limited individual roles *in vivo*, the decrease in levels of wild-type protein due to the formation of alternately spliced forms may decrease receptor function, and this may be an additional level of regulation of receptor transactivation. The variation in expression levels of the different splice variants may result in individual differences in transactivation, and this should be further studied to help understand the role that alternatively spliced variants of these receptors play in the overall transactivation of the receptors.

Different proteins within a cell, including variant proteins generated from a single gene, may degrade at different rates within the cell. As such, the mRNA levels of variants may not reflect the expression levels of the protein products. In our study, we carried out transient transfection experiments involving splice variants of nuclear receptors using levels of plasmids that were within the physiological levels of mRNA as determined by realtime PCR. As such, the expression of protein product from a specific inclusion level of plasmid should still reflect a similar *in vivo* expression level of the variant protein, assuming that the degradation rate is similar between cell lines and primary cells. Further support for this rationale should be gathered in future studies, employing antibodies specific to porcine receptor orthologs.

Since pgPXR-WT and pgFXR-WT were the variants that contained the conserved nuclear receptor domains that most closely resembled hPXR and hFXR, these variants were used to test the ligand complement of porcine PXR and FXR. The human orthologs of each were also tested with the same set of ligands, to allow direct comparison of human and pig PXR and FXR. The ligands chosen included known hPXR or hFXR activators, and common steroid hormones and endogenous compounds found in high concentrations in some pigs, including skatole and its metabolites, as well as androstenone and its precursors and metabolites. Of the 22 ligands tested, pgPXR-WT and hPXR responded to 13; of these, 12 acted as agonists for both PXR orthologs. Both the drug rifampicin as well as several steroids, including pregnenolone, progesterone, testosterone, 5β-DHT, 5α-DHT and estradiol, activated hPXR in this study, which is in agreement with previous studies.[14,32] These ligands also significantly activated pgPXR-WT, and the response of both PXR orthologs to progesterone, testosterone and the estrogens (E1, E1S and E2) was comparable, indicating a degree of conservation of ligand specificity between hPXR and pgPXR-WT. However, pgPXR-WT also significantly responded to treatment with PCN, which has been shown to act as an agonist for mouse, rat and rabbit PXR, but not human PXR.[38] Human PXR also significantly responded to a larger number of androgens than did pgPXR-WT.

The differential ligand profiles for the human and pig orthologs of PXR are likely due to changes to key residues within the ligand binding pocket. The ligand binding pocket of hPXR is made up of 28 key residues,[39] 20 of which are hydrophobic, six are polar and two are charged.
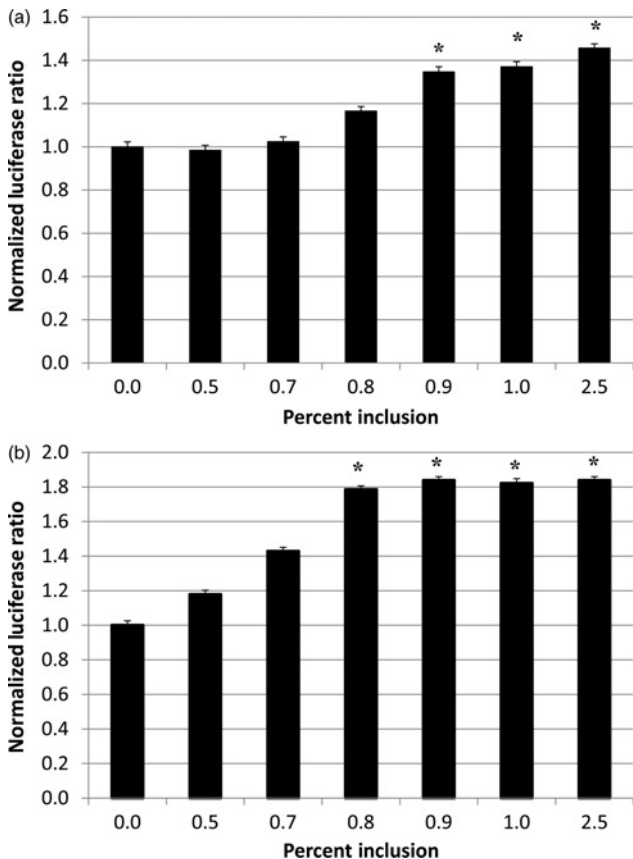
In pgPXR, methionine 243 is altered to an isoleucine, a change that does not alter the net charge or polarity of this position, although the alteration of side chains may alter the shape of the binding pocket. The second alteration does result in the loss of a polar residue, with threonine 311 being substituted by a proline. The loss of this polar group, which will be involved in forming interactions with polar regions of ligands, may alter the ability of the ligand pocket to interact with certain ligands.

A smaller number of tested ligands resulted in activation of either pgFXR-WT or hFXR. Each was activated by three ligands, with two shared between them, namely CDCA, a bile acid and GW4064, a synthetic ligand, both of which have been shown previously to cause hFXR transactivation.[4,9,40] GW4064 was a more potent hFXR agonist than CDCA, which agrees with previous studies.[40] In pigs, the reverse is true, with CDCA being a more potent agonist than GW4064. This suggests that there has been a divergence within the FXR LBD between hFXR and pgFXR-WT, resulting in different ligand specificity. This is further supported by the third agonist for each ortholog, with pgFXR-WT showing a response with progesterone treatment, while hFXR responds to LCA. The differences between hFXR and pgFXR-WT ligand profiles are not caused by alterations in key ligand binding residues, for none of these are changed between the two orthologs. Rather, other residue changes within the LBD of pgFXR-WT compared with hFXR likely cause protein folding differences, resulting in different ligand specificities.

Skatole was identified as a significant antagonist of both pgPXR-WT and pgFXR-WT, decreasing their activities by up to 36% and 58%, respectively. Skatole also decreased the constitutive transactivation of pgCAR by up to 23%. This effect was dose-dependent, with significant decreases in pgPXR-WT and pgCAR transactivation occurring with 1 μmol/L skatole treatment, while pgFXR-WT had a significant decrease in transactivation beginning at the 5 μmol/L skatole treatment level. This dose-dependent inhibition was also seen for the human orthologs of these three receptors. Significant inhibition of hPXR and hCAR first occurred with 2.5 μmol/L skatole treatment, while hFXR was first inhibited at 0.25 μmol/L skatole. Maximal inhibition of hPXR, hCAR, and hFXR was found to occur at 10 μmol/L, 5 μmol/L, and 5 μmol/L, respectively, with decreases of 41%, 13% and 48% being seen. Skatole is a tryptophan degradation product generated by microflora in the gut.[41,42] In ruminants, skatole has been shown to be a pneumotoxin, due to formation of a DNA adduct after metabolism by a lung-specific cytochrome P450 (CYP2F1 in humans;[43,44]). This effect is not seen in pigs, where skatole is instead absorbed into fat deposits and contributes to boar taint, an unpleasant odor released from pig fat with negative effects on meat quality.[45] The hepatic metabolism and clearance of skatole is inhibited by androstenone, the other component of boar taint.[46,47] The repression of pgPXR-WT and pgFXR-WT, as well as pgCAR-WT may limit the expression of enzymes involved in the metabolism of androstenone and skatole. As such, the downstream effects of receptor activation should be studied, to determine what metabolic genes are controlled by which receptor.

These studies will help determine how each receptor may be involved in the control of boar taint, as well as to determine the interplay between different receptors that are affected by a single ligand, such as the activation of pgPXR-WT by 5β-DHT and the inhibition of pgCAR-WT by the same ligand.[26]

The potential effects of pgPXR alternatively spliced variants on the transactivation of pgPXR-WT were tested using a dual-luciferase reporter assay system. The five alternatively spliced variants had no individual transactivation when treated with rifampicin. However, pgPXR-SV1 had a dose-dependent dominant-positive effect on the transactivation of pgPXR-WT; this occurred over a physiological range of expression levels measured in this work. An estrogen receptor splice variant lacking a functional LBD but retaining active DNA binding and AF-1 and AF-2 domains was shown to exert a significant dominant-positive effect on wild-type ERα.[27] These authors suggest that this dimer pair binds to the ER response element in a more stable manner than an ERα/ERα homodimer, resulting in constitutive activation of target genes. With recent evidence suggesting that PXR may be capable of forming functional heterotetramers between PXR/RXR heterodimers,[48] pgPXR-SV1 may exert its effect through a similar mechanism as the ER dominant-positive variant. This concept is supported by the fact that pgPXR-SV1 caused a significant increase in pgPXR-WT transactivation even in the absence of an activating or inhibiting ligand. However, the degree to which the transactivation of pgPXR-WT increased cannot be solely explained by ligand-independent transactivation, for this amounts to an increase in the dual-luciferase ratio of 0.12 at the 2.5% inclusion level (Figure 9), which is only 14% of the increase in pgPXR-WT transactivation due to pgPXR-SV1. Thus, the dominant-positive effect may be caused by an increase in the time which the ligand activated wild-type receptor is bound to response elements in gene promoter regions.

Of the pgFXR alternatively spliced variants, only pgFXR-SV1 retained transactivation, as was expected based on a study of a hFXR variant containing the same four amino acid insertion.[35] Unlike the human ortholog of this variant, pgFXR-SV1 retained transactivation that was not significantly different from the transactivation of pgFXR-WT. This difference between the human and pig variants may be due to alterations in protein folding between the orthologs, resulting in a less appreciable effect of the insert in pgFXR-SV1. Altered protein folding is also a viable explanation for the lack of transactivation seen with the other pgFXR variants. pgFXR-SV2, pgFXR-SV4 and pgFXR-SV5 retained intact ligand binding and AF-2 domains, and as such altered ligand specificity or co-repressor binding affinity would not be expected. The removal of portions of the hinge regions of these proteins would likely cause significant alterations to their tertiary structures, thereby abolishing transactivation. pgFXR-SV3 also lacked transactivation, which was expected based on the loss of the AF-2 domain and the majority of the LBD.

The transactivation of pgFXR-SV1 was also tested in a system expressing hFXR in place of pgFXR. It was found that the increase in transactivation with hFXR was due to the individual transactivation of pgFXR-SV1, rather than a dominant-positive effect. As such, the increase in

transactivation caused by pgFXR-SV1 is specific to pgFXR-WT, and appears to be synergistic. As with the pgPXR dominant-positive variants, a component of the increase in transactivation may be caused by an inferred level of ligand-independent transactivation; however, this makes up only 14% of the increase. The remainder of the increase is likely ligand dependent, and may be due to an extended duration of time the activated receptor complex is bound to DNA response elements compared with the wild-type pgFXR on its own. Since both pgPXR and pgFXR dominant-positive variants increase inferred ligand-independent transactivation by a similar degree, the presence of these variants may be a mechanism for maintaining some constitutive transactivation of these receptors. The lack of effect of pgFXR-SV1 on hFXR transactivation may be explained by the divergence of the N-terminal end of the protein, which includes the AF-1 domain. This domain is involved in co-regulator protein binding,[49] and as such differences between these domains in any hypothetical tetramer may alter the recruitment of these accessory proteins, causing a loss of the pgFXR-SV1 dominant-positive effect.

In order to more closely mimic *in vivo* conditions on the dominant-positive effects of pgPXR-SV1 and pgFXR-SV1, these receptors were co-transfected along with their corresponding wild-type receptors, as well as all of the other splice variants found for the corresponding receptor. This was done to ensure that the dominant-positive effects seen would be likely to occur *in vivo*, where all splice variants were present. Each variant was expressed at the maximal inclusion level seen with realtime PCR, to generate optimal conditions for potential interference of the dominant-positive effects to occur. It was found that the presence of the other splice variants for each receptor did not interfere with the dominant-positive effects of pgPXR-SV1 or pgFXR-SV1; this indicates that the dominant-positive effect could potentially occur in the presence of the other splice variants.

The effects of the two dominant-positive splice variants, pgPXR-SV1 and pgFXR-SV1, on skatole inhibition of the wild-type receptors were also investigated. It was found that both pgPXR-SV1 and pgFXR-SV1 reversed the skatole inhibitory effect on their corresponding wild-type receptor, doing so within their *in vivo* expression levels. This confirms that the inhibitory effects of skatole are not due to cellular toxicity. These effects of the dominant-positive variants may point towards an *in vivo* role as a means of overcoming inhibition of the wild-type receptors by an inhibitory xenobiotic, such as skatole, that would normally decrease receptor function, thus likely decreasing its own metabolic clearance. The dominant-positive effects of certain receptor variants, such as pgPXR-SV1, may act to overcome this inhibition, allowing for normal skatole metabolism and clearance to occur.

Each of the dual-luciferase assays carried out in this study should also be carried out in other expression systems. This would ensure that the effects seen, either activation of wild-type nuclear receptors or dominant effects from splice variants, were not just artefacts of the expression system and culture conditions used here. The new system used could involve using new stable cell lines, or a new reporter plasmid, or a combination of both. Also, these assays should be carried out using primary cells, specifically porcine hepatocytes, as the expression system to more closely represent the *in vivo* system, and using defined media that does not contain potentially interfering compounds present in fetal bovine serum.

The purpose of this study was to characterize the porcine homologues of PXR and FXR, along with their splice variants. Further research should be carried out to determine the downstream effects of activation of these nuclear receptors in pigs, and if this results in altered physiological conditions that mimic alterations seen in humans upon activation of the same receptors. This information would be a valuable tool for employing pigs as a model for humans in research. The levels of the pgPXR and pgFXR splice variants should also be studied in a larger and more varied population, covering a larger variety of pig breeds. This might uncover individuals with greater levels of individual pgPXR or pgFXR splice variants, which may indicate specific roles these variants could play in regulating physiological processes and diseases.

In conclusion, pgFXR is highly homologous to hFXR in the major functional domains, although there is little homology at the extreme N-terminus. The orthologs retain a degree of similar transactivation, with two agonists activating both orthologs. pgPXR-WT responded to 13 ligands, 12 of which were shown to be agonists of hPXR. One ligand tested, skatole, was found to be a significant antagonist of pgFXR-WT, pgPXR-WT and pgCAR-WT. Both pgPXR-WT and pgFXR-WT have five alternatively spliced variants that were tested for expression levels and transactivation. The pgPXR variants comprised of 5.33% of total pgPXR on average, with pgPXR-SV5 being the most prevalent and pgPXR-SV2 the least. Two of the five pgPXR variants increased pgPXR-WT transactivation in co-transfection experiments with rifampicin treatment, although none of the pgPXR variants responded to rifampicin treatment individually. The pgFXR variants were identified as part of this study, and comprised 6.01% of total pgFXR on average. pgFXR-SV2 was the most prevalent pgFXR variant while pgFXR-SV4 was the least prevalent. Only pgFXR-SV1 was shown to have any transactivation with CDCA treatment individually. pgFXR-SV1 also had a dominant-positive effect when co-transfected with pgFXR-WT. Further mechanistic studies investigating these positive dominant effects are warranted.

REFERENCES

1 Francis GA, Fayard E, Picard F, Auwerx J. Nuclear receptors and the control of metabolism. *Annu Rev Physiol* 2003;**65**:261–311

2 Laudet V, Hänni C, Coll J, Catzeflis F, Stéhelin D. Evolution of the nuclear receptor gene superfamily. *EMBO J* 1992;**11**:1003–13

3 Mangelsdorf DJ, Thummel C, Beato M, Herrlich P, Schütz G, Umesono K, Blumberg B, Kastner P, Mark M, Chambon P, Evans RM. The nuclear receptor superfamily: the second decade. *Cell* 1995;**85**:835–9

4 Makishima M, Okamoto AY, Repa JJ, Tu H, Learned RM, Luk A, Hull MV, Lustig KD, Mangelsdorf DJ, Shan B. Identification of a nuclear receptor for bile acids. *Science* 1999;**284**:1362–5

5 Wang S, Lai K, Moy FJ, Bhat A, Hartman HB, Evans MJ. The nuclear receptor farnesoid X receptor (FXR) is activated by androsterone. *Endocrinology* 2006;**147**:4025–33

6 Song CS, Echchgadda I, Baek BS, Ahn SC, Oh T, Roy AK, Chatterjee B. Dehydroepiandrosterone sulfotransferase gene induction by bile acid activated farnesoid X receptor. *J Biol Chem* 2001;**276**:42549–56

7 Sinclair PA, Gilmore WJ, Lin Z, Lou Y, Squires EJ. Molecular cloning and regulation of porcine SULT2A1: relationship between SULT2A1 expression and sulfoconjugation of androstenone. *J Mol Endocrinol* 2006;**36**:301–11

8 Jung D, Mangelsdorf DJ, Meyer UA. Pregnane X receptor is a target of farnesoid X receptor. *J Biol Chem* 2006;**281**:19081–91

9 Park DJ, Blanchard SG, Bledsoe RK, Chandra G, Consler TG, Kliewer SA, Stimmel JB, Willson TM, Zavacki AM, Moore DD, Lehmann JM. Bile acids: natural ligands for an orphan nuclear receptor. *Science* 1999;**284**:1365–8

10 Bookout AL, Jeong Y, Downes M, Yu RT, Evans RM, Mangelsdorf DJ. Anatomical profiling of nuclear receptor expression reveals a hierarchical transcriptional network. *Cell* 2006;**126**:789–99

11 Watkins RE, Wisely GB, Moore LB, Collins JL, Lambert MH, Williams SP, Willson TM, Kliewer SA, Redinbo MR. The nuclear xenobiotic receptor PXR: structural determinants of directed promiscuity. *Science* 2001;**292**:2329–33

12 Moore LB, Parks DJ, Jones SA, Bledsoe RK, Consler TG, Stimmel JB, Goodwin B, Liddle C, Blanchard SG, Willson TM, Collins JL, Kliewer SA. Orphan nuclear receptors constitutive androstane receptor and pregnane X receptor share xenobiotic and steroid ligands. *J Biol Chem* 2000;**275**:15122–7

13 Moore JT, Moore LB, Maglich JM, Kliewer SA. Functional and structural comparison of PXR and CAR. *Biochim Biophys Acta* 2003;**1619**:235–8

14 Blumberg B, Sabbagh W Jr, Juguilon H, Bolado J Jr, van Meter CM, Ong OS, Evans RM. SXR, a novel steroid and xenobiotic-sensing nuclear receptor. *Genes Dev* 1998;**12**:3195–205

15 Duanmu Z, Locke D, Smigelski J, Wu W, Dahn MS, Falany CN, Kocarek TA, Runge-Morris M. Effects of dexamethasone on aryl (SULT1A1)- and hydroxysteroid (SULT2A1)-sulfotransferase gene expression in primary cultured human hepatocytes. *Drug Metab Dispos* 2002;**30**:997–1004

16 Knight TR, Choudhuri S, Klaassen CD. Induction of hepatic glutathione-*S*-transferases in male mice by prototypes of various classes of microsomal enzyme inducers. *Toxicol Sci* 2008;**106**:329–38

17 Pollock CB, Rogatcheva MB, Schook LB. Comparative genomics of xenobiotic metabolism: a porcine-human PXR gene comparison. *Mamm Genome* 2007;**18**:210–9

18 Choi H-S, Chung M, Tzameli I, Simha D, Lee Y-K, Seol W, Moore DD. Differential transactivation by two isoforms of the orphan nuclear hormone receptor CAR. *J Biol Chem* 1997;**272**:23565–71

19 Auerbach SS, Ramsden R, Stoner MA, Verlinde C, Hassett C, Omiecinski CJ. Alternatively spliced isoforms of the human Constitutive Androstane Receptor. *Nucleic Acids Res* 2003;**31**:3194–207

20 Auerbach SS, Stoner MA, Su S, Omiecinski CJ. Retinoid X receptor-α-dependent transactivation by a naturally occurring structural variant of human constitutive androstane receptor (NRI13). *Mol Pharmacol* 2005;**69**:1239–53

21 Jinno H, Tanaka-Kagawa T, Hanioka N, Ishida S, Saeki M, Soyama A, Itoda M, Nishimura T, Saito Y, Ozawa S, Ando M, Sawada J. Identification of novel alternative splice variants of human constitutive androstane receptor and characterization of their expression in the liver. *Mol Pharmacol* 2004;**65**:496–502

22 Savkur RS, Wu Y, Bramlett KS, Wang M, Yao S, Perkins D, Totten M, Searfoss G, Ryan TP, Su EW, Burris TP. Alternative splicing within the ligand binding domain of the human constitutive androstane receptor. *Mol Genet Metab* 2003;**80**:216–26

23 Herskowitz I. Functional inactivation of genes by dominant negative mutations. *Nature* 1987;**329**:219–22

24 Kocarek TA, Shenoy SD, Mercer-Haines NA, Runge-Morris M. Use of dominant negative nuclear receptors to study xenobiotic-inducible gene expression in primary cultured hepatocytes. *J Pharmacol Toxicol Methods* 2002;**47**:177–87

25 Agostini M, Schoenmakers E, Mitchell C, Szatmari I, Savage D, Smith A, Rajanayagam O, Semple R, Luan J, Bath L, Zalin A, Labib M, Kumar S, Simpson H, Blom D, Marais D, Schwabe J, Barraso I, Trembath R, Wareham N, Nagy L, Gurnell M, O'Rahilly S, Chatterjee K. Non-DNA binding, dominant-negative, human PPARγ mutations cause lipodystrophic insulin resistance. *Cell Metab* 2006;**4**:303–11

26 Gray MA, Peacock JN, Squires EJ. Characterization of the porcine constitutive androstane receptor (CAR) and its splice variants. *Xenobiotica* 2009;**39**:915–30

27 Chaidarun SS, Alexander JM. A tumor-specific truncated estrogen receptor splice variant enhances estrogen-stimulated gene expression. *Mol Endocrinol* 1998;**12**:1355–66

28 Schook L, Beattie C, Beever J, Donovan S, Jamison R, Zuckerman F, Niemi S, Rothschild M, Rutherford M, Smith D. Swine in biomedical research: Creating the building blocks of animal models. *Anim Biotechnol* 2005;**16**:183–90

29 Livak KJ, Schmittgen TD. Analysis of relative gene expression data using real-time quantitative PCR and the 2(-delta delta C(T)) method. *Methods* 2001;**25**:402–8

30 Squires EJ, Sueyoshi T, Negishi M. Cytoplasmic localization of pregnane X receptor and ligand-dependent nuclear translocation in mouse liver. *J Biol Chem* 2004;**279**:49307–14

31 Jung D, Podvinec M, Meyer UA, Mangelsdorf DJ, Fried M, Meier PJ, Kullak-Ublick GA. Human organic anion transporting polypeptide 8 promoter is transactivated by the farnesoid X receptor/bile acid receptor. *Gastroenterology* 2002;**122**:1954–66

32 Goodwin B, Hodgson E, Liddle C. The orphan human pregnane X receptor mediates the transcriptional activation of CYP3A4 by rifampicin through a distal enhancer module. *Mol Pharmacol* 1999;**56**:1329–39

33 Wang H, Faucette SR, Gilbert D, Jolley SL, Sueyoshi T, Negishi M, LeCluyse EL. Glucocorticoid receptor enhancement of pregnane x receptor-mediated CYP2B6 regulation in primary human hepatocytes. *Drug Metab Dispos* 2003;**31**:620–30

34 Reschly EJ, Ai N, Ekins S, Welsh WJ, Hagey LR, Hofmann AF, Krasowski MD. Evolution of the bile salt nuclear receptor FXR in vertebrates. *J Lipid Res* 2008;**49**:1577–87

35 Wu C, Orozco C, Boyer J, Leglise M, Goodale J, Batalov S, Hodge CL, Haase J, Janes J, Huss JW III, Su AI. BioGPS: an extensible and customizable portal for querying and organizing gene annotation resources. *Genome Biol* 2009;**10**:R130

36 Su AI, Wiltshire T, Batalov S, Lapp H, Ching KA, Block D, Zhang J, Soden R, Hayakawa M, Kreiman G, Cooke MP, Walker JR, Hogenesch JB. A gene atlas of the mouse and human protein-encoding transcriptomes. *Proc Natl Acad Sci USA* 2004;**101**:6062–7

37 Huber RM, Murphy K, Miao B, Link JR, Cunningham MR, Rupar MJ, Gunyuzlu PL, Haws TF, Kassam A, Powell F, Hollis GF, Young PR, Mukherjee R, Burn TC. Generation of multiple farnesoid-X-receptor isoforms through the use of alternative promoters. *Gene* 2002;**290**: 35–43

38 Jones SA, Moore LB, Shenk JL, Wisely GB, Hamilton GA, McKee DD, Tomkinson NC, LeCluyse EL, Lambert MH, Willson TM, Kliewer SA, Moore JT. The pregnane X receptor: a promiscuous xenobiotic receptor that has diverged during evolution. *Mol Endocrinol* 2000;**14**:27–39

39 Östberg T, Bertilsson G, Jendeberg L, Berkenstam A, Uppenberg J. Identification of residues in the PXR ligand binding domain critical for species specific and constitutive activation. *Eur J Biochem* 2002;**269**:4896–904

40 Maloney PR, Parks DJ, Haffner CD, Fivush AM, Chandra G, Plunket KD, Creech KL, Moore LB, Wilson JG, Lewis MC, Jones SA, Wilson TM. Identification of a chemical tool for the orphan nuclear receptor FXR. *J Med Chem* 2000;**43**:2971–4

41 Yokoyama MT, Carlson JR. Microbial metabolites of tryptophan in the intestinal tract with special reference to skatole. *Am J Clin Nutr* 1979;**32**:173–8

42 Jensen MT, Cox RP, Jensen BB. 3-methylindole (skatole) and indole production by mixed populations of pig fecal bacteria. *Appl Environ Microbiol* 1995;**61**:3180–4

43 Deslandes B, Gariepy C, Houde A. Review of microbiological and biochemical effects of skatole on animal production. *Livest Prod Sci* 2001;**71**:193–200

44 Nichols WK, Mehta R, Skordos K, Mace K, Pfeifer AMA, Carr BA, Minko T, Burchial SW, Yost GS. 3-methylindole-induced toxicity to human bronchial epithelial cell lines. *Toxicol Sci* 2003;**71**:229–36

45 Baek C, HansenMoller J, Friis C, Cornett C, Hansen SH. Identification of selected metabolites of skatole in plasma and urine from pigs. *J Agric Food Chem* 1997;**45**:2332–40

46 Zamaratskaia G, Gilmore WJ, Lundström K, Squires EJ. Effect of testicular steroids on catalytic activity of cytochrome P450 enzymes in porcine liver microsomes. *Food Chem Toxicol* 2007;**45**:676–81

47 Doran E, Whittington FW, Wood JD, McGivan JD. Cytochrome P450IIE1 (CYP2E1) is induced by skatole and this induction is blocked by androstenone in isolated pig hepatocytes. *Chem Biol Interact* 2002;**140**:81–92

48 Noble SM, Carnahan VE, Moore LB, Luntz T, Wang H, Ittoop OR, Stimmel JB, Davis-Searles PR, Watkins RE, Wisely GB, LeCluyse E, Tripathy A, McDonnell DP, Redinbo RM. Human PXR forms tryptophan zipper-mediated homodimer. *Biochemistry* 2006;**45**:8579–89

49 Wärnmark A, Treuter E, Wright AP, Gustafsson JA. Activation function 1 and 2 of nuclear receptors: molecular strategies for transcriptional activation. *Mol Endocrinol* 2003;**17**:1901–9